Cingulate and Cerebellar Beta Oscillations are Engaged in the Acquisition of Auditory-Motor Sequences

Abbreviated title: Beta oscillations during sensorimotor learning

María Herrojo Ruiz*[a,b], Burkhard Maess[c], Eckart Altenmüller[d], Gabriel Curio[a,e], Vadim Nikulin[a,f,g]

[a]Neurophysics Group, Department of Neurology, Campus Benjamin Franklin, Charité-University Medicine Berlin, Berlin 12203, Germany

[b]Department of Psychology, Whitehead Building, Goldsmiths, University of London, London SE14 6NW, UK

[c]Research and Development Unit "Magnetoencephalography", Max Planck Institute for Human Cognitive and Brain Sciences, D-04103 Leipzig, Germany

[d]Institute of Music Physiology and Musicians' Medicine, Hanover University of Music, Drama, and Media, Hanover, Germany

[e]Bernstein Center for Computational Neuroscience, Berlin 10115, Germany

[f]Department of Neurology, Max Planck Institute for Human Cognitive and Brain Sciences, D-04103 Leipzig, Germany

[g]Center for Cognition and Decision making, National Research University Higher School of Economics, Russian Federation.

***Corresponding author:** Dr. María Herrojo Ruiz, Department of Psychology, Whitehead Building, Goldsmiths, University of London, Lewisham Way, New Cross, London SE14 6NW, UK; M.Herrojo-Ruiz@gold.ac.uk,; Phone: +44 20 7896 2667

Number of figures and tables: 7

Number of pages: 51 pages (including this one).

Keywords: oscillations, sensorimotor learning, error-monitoring, cingulate cortex, cerebellum

Abstract

Singing, music performance and speech rely on the retrieval of complex sounds, which are generated by the corresponding actions and are organized into sequences. It is crucial in these forms of behavior that the serial organization (i.e., order) of both the actions and associated sounds be monitored and learned. To investigate the neural processes involved in the monitoring of serial order during the initial learning of sensorimotor sequences, we performed magnetoencephalographic recordings while participants explicitly learned short piano sequences under the effect of occasional alterations of auditory feedback (AAF). The main result was a prominent and selective modulation of beta (13-30Hz) oscillations in cingulate and cerebellar regions during the processing of AAF that simulated serial order errors. Furthermore, the AAF-induced modulation of beta oscillations was associated with higher error rates, reflecting compensatory changes in sequence planning. This suggests that cingulate and cerebellar beta oscillations play a role in tracking serial order during initial sensorimotor learning and in updating the mapping of the sensorimotor representations. The findings support the notion that the modulation of beta oscillations is a candidate mechanism for the integration of sequential motor and auditory information during an early stage of skill acquisition in music performance. This has potential implications for singing and speech.

Music performance, as well as song and speech, is a paradigmatic example of sensorimotor learning, that is, the monitoring of auditory feedback and its modulation of motor control (Brown and Palmer, 2012; Zatorre et al., 2007). Singing and music performance require a particularly high temporal and spectral precision of the auditory output, thereby making increased demands on sensorimotor control compared to speech (Natke et al., 2003; Patel, 2011; Tierney et al., 2013; Zatorre and Baum, 2012).

An essential feature of these types of behavior is their sequential nature: The events (chords, notes or vowels) have to be accurately produced in a specific temporal (serial) order in which the related actions follow each other. How the brain encodes serial order has been a fundamental question since Lashley's seminal work on the organization of sequential behavior (Lashley, 1951). A positional account for serial order, in which the position of the items within a sequence is coded as a separate representation, has been demonstrated in short and long-term memory, as well as in motor learning (for a recent review see Dehaene et al., 2015). Specifically, neurophysiological evidence primarily from non-human primates supports the involvement of the anterior cingulate cortex (ACC), supplementary motor areas (SMA), and prefrontal cortices in the separate coding of serial order (Amiez et al., 2007; Averbeck et al., 2002; Clower and Alexander, 1998; Ninokura et al., 2004; Nieder et al., 2012; Procyk and Joseph, 2001). There is, however, sparse evidence with regard to the neural mechanisms for serial-order coding during the learning

of auditory-motor associations in the context of music performance and singing. Here we hypothesize that in these types of behavior, dedicated neural mechanisms should monitor both the auditory and motor sources of information with regard to the serial order of the produced actions, particularly during the initial learning. To date, this hypothesis has remained largely untested.

The primary goal of our study was to investigate the neural mechanisms underlying the monitoring of serial order during sensorimotor sequence learning as revealed by alterations of auditory feedback (AAF). To that aim, we recruited 21 participants whose task it was to explicitly learn short movement sequences on a digital piano while listening to the corresponding auditory feedback. At the behavioral level, we hypothesized that AAF would have a different impact on the ongoing performance depending on whether AAF activated incorrect serial positions within the sequence. Data from previous behavioral studies on this matter are contentious. Some studies focusing on piano performance show a disruption in the accuracy of sequencing due to serial shifts of feedback (pitch error rates increase, Pfordresher and Palmer, 2006). However, other studies using random pitch alterations, including manipulations with serial shifts of feedback, have not found changes in the error rates or other types of behavioral adaptation (Maidhof et al., 2010). Therefore, the extent to which auditory-feedback-based alterations of the serial order of actions disrupts learning remains to be understood. To further clarify this matter, the present study used AAF of two kinds: AAF simulating serial order errors (alterations of serial order or ASO) and AAF with pitch values that were unrelated to the sequence contents (unrelated auditory feedback or UAF).

Until now almost all neuroimaging studies investigating the effects of AAF did not use pitch

alterations that interfered with the serial order of the actions in the sequence (Chang el al, 2013; Maidhof et al., 2010; Tourville et al., 2008; Zarate and Zatorre, 2008). One notable exception is the functional magnetic resonance imaging (fMRI) study by Pfordresher and colleagues (2014), which used six different kinds of AAF after their pianist subjects undertook initial training on piano melodies. This study revealed an involvement of the premotor cortex in processing delayed auditory feedback (temporal shift), and an engagement of the cerebellum and ACC in processing serially shifted feedback. In addition, the superior temporal gyrus was involved in processing both kinds of AAF. What remain to be investigated, however, are the neural mechanisms that update the mapping of the sensorimotor representations following serial shifts in auditory feedback during initial learning.

Elucidating the neural mechanisms involved in monitoring the acquisition of the serial order of actions during sensorimotor learning requires a time-resolved technique with a millisecond resolution. This high temporal accuracy is relevant in the context of the fast movement rates that characterize music or singing performance (e.g., eight notes per second, Herrojo Ruiz et al. 2009). Consequently, we used magnetoencephalography (MEG) to track the fast changes in neuronal oscillatory activity following AAF and to assess the neural generators engaged in monitoring the different kinds of AAF.

Two strong candidates for a neurophysiological signature of processing auditory-feedback alterations during sensorimotor learning are theta (4-7 Hz) and beta (13-30Hz) oscillations. Oscillatory activity in the theta frequency range across medial frontal or cingulate regions has been consistently associated with the processing of correct or incorrect feedback signaling an error in

the performance (Cavanagh et al., 2011; Luft, 2014, Nieuwenhuis et al., 2004). The main factor influencing frontal midline theta might be outcome probability, which is primarily associated with the non-phase-locked (induced) portion of theta oscillations (Hajihosseini and Holroyd, 2013). Beta oscillations are crucial during sensorimotor learning and performance, as reflected in their involvement in processing self-produced pitch errors in piano performance (Herrojo Ruiz et al., 2011), or in sensorimotor adaptation (Tan et al., 2014; Torrecillos et al., 2015). In addition, there is vast evidence linking changes in beta oscillations to the processing of different aspects of movements, such as movement-related cues, boundary elements of sensorimotor sequences or temporal intervals (Bartolo et al., 2014; Herrojo Ruiz et al., 2014a; Iversen et al., 2009; Leventhal et al., 2012; Oswal et al., 2012).

Our specific hypotheses at the neural level were (see aforementioned references for anatomical candidates): (1) theta-band oscillations are engaged in monitoring alterations of auditory feedback of any kind (ASO and UAF); (2) beta-band oscillations specifically reflect the processing of auditory feedback alterations of the serial order; (3) a potential dissociation between the spectral content of oscillatory activity induced by processing AAF of the ASO or UAF kind is reflected in different patterns of neuronal sources located in the temporal, cingulate, prefrontal, SMA and cerebellar regions

Methods

Participants

21 participants (10 females, median age 27 [ranging from 22 to 34] years; data after exclusion of 1 participant, see below) who had no intensive piano training (accumulated lifetime practice

experience below 500 hours) participated in the study. All participants were right handed (Handedness score median 100, range 60 to 100; Oldfield 1971), had no history of neurological or psychiatric disease and received remuneration for their participation. One participant was discarded from further analysis due to artifacts in MEG signals. of the study. Written informed consent was obtained from each participant before the experiment that was approved by the local ethics committee.

Material and Apparatus

Six different piano sequences of length between four and six notes and with isochronous timing (1 keystroke every 300 ms) were used for this study. The pitch content for each sequence was limited to the pitch values available in the MEG-compatible keyboard, which were B, C, $C^{\#}$, D; these pitch values corresponded to MIDI note numbers 60, 61, 62, 63 (**Figure 1**). The sequences were designed to enable different combinations of transitions between successive finger movements.

Participants had to perform the piano sequences with their dominant (right) hand on a custom-made keyboard, which was formerly part of an actual acoustic Grand Piano keyboard. Auditory feedback was delivered following standard procedure in MEG recordings through air-conducting plastic ear tubes. The keyboard had been stripped off any ferromagnetic component and tested for MEG and MRI compliance (Bangert et al., 2006). It was connected via optical fibers to an electronic processor outside the MEG room, where the signal was A/D-converted and translated into a standard serial interface protocol (Musical Instrument Digital Interface, MIDI). Performance information as provided by the MIDI device included time onsets of keystrokes

relative to the previous event (inter-onset-interval or IOI [ms]), MIDI note numbers that correspond to the pitch, and MIDI velocities (in arbitrary units, a.u.). Alterations of auditory feedback (AAF) and behavioral data acquisition were conducted using the software Visual Basic (MIDI libraries) on a Windows Notebook. The time delay between keystrokes when registered as MIDI data and the corresponding trigger in the MEG recording was in the range of 20-25 ms. This delay was corrected in the subsequent MEG analysis.

_____ Figure 1 around here _____

Procedure

Participants were explicitly taught the sequence contents and the (most comfortable) digit-to-tone mapping they should use. Before recording of the performance or MEG data, participants had to briefly practice each sequence until an error-free performance was achieved at a self-defined tempo for five consecutive renditions.

There was a familiarization (training) and subsequent performance session. Both these sessions can be considered to relate to the early stage of motor skill learning as described in previous studies. The hallmarks of the early motor skill learning stage are the rapid improvements in performance (i.e. improved timing and reduced error rates; Dayan and Cohen, 2011).

During the *familiarization* session participants completed one training block consisting of three trials of 23s-duration for each sequence type. In each trial, participants continuously practiced a given sequence type while listening to the corresponding auditory feedback. Performance tempo was induced by using a synchronization-continuation paradigm, that is, the

tempo was paced prior to each trial by a metronome at 200 beats per minute (bpm, 1 keystroke every 300 ms; **Figure 1**). The metronome was turned off before the trial onset. The aim of this training condition was to ensure that participants knew the correct serial order of the actions for each sequence type to be able to play them from memory in the subsequent session of MEG recording. In addition, we expected that this session (lasting less than 1 minute of practice per sequence type) would lead to rapid improvements in performance (Dayan and Cohen, 2011).

In the *performance* session, one block of 15 trials of 23s-duration had to be completed for each sequence-type (~5-6 min per sequence type). Prior to each trial, the tempo was again induced by a metronome at 200 bpm. During performance, participants listened to the auditory feedback associated to the key presses. They were instructed to play repeatedly the sequence several times during the trial without pause. In this session we recorded MEG during performance. Participants were instructed to focus their eyes at a central fixation point on the screen during playing and, in between-trials, to focus on the visual cues at the center of the screen.

The control condition was constituted by trials 1, 6 and 11, in which the auditory feedback corresponding to each key press was not modified. Alterations of auditory feedback (AAF) were introduced in the remaining trials, and they were dissociated into two types of alterations corresponding to two experimental conditions. Auditory-feedback based alterations of serial order (ASO) were introduced in trials 2, 4, 8, 10, 12, 14. AAF with pitch values that did not correspond to the sequence contents (unrelated auditory feedback or UAF; with pitch values $A^{\#}$ or $D^{\#}$, and MIDI note numbers 59 and 64; Note that these pitch values were one semitone lower or higher than the lowest or highest pitch values contained in the sequences, respectively; see **Figure**

1) were introduced in trials 3, 5, 7, 9, 13, 15. In the experimental conditions, the AAF was introduced randomly between every 8th and 10th produced note (every 8.37 [0.05] keystrokes on average). We used this design because lower AAF rates do not lead to behavioral effects (Maidhof et al., 2010; Pfordresher and Kulpa, 2011). The specifications of each trial within a sequence-type-specific block for the familiarization and performance sessions are given in **Figure 1.**

At the end of the experiment, participants were asked to complete a questionnaire that aimed to assess their estimation of rates of self-produced errors in the control condition and the experimental conditions with AAF as well as their awareness of the different types of feedback (further details are provided in the **Supplementary Material** available online).

Performance Analysis

General performance was evaluated in terms of average timing (IOI), temporal variability (coefficient of variation, CV, of IOI), pitch error rate and average keystroke velocity. Note that MIDI velocity is related to the loudness of the keystroke. With the exception of the error rate, all analyses were performed on events with "adequate" temporal properties (an IOI lower than 1000 ms to exclude extreme outliers related to pauses – if any – during performance) and which were not surrounded by performance errors (at least within three preceding and following keystrokes). This set of events was the basis of the trials for later MEG analyses. Behavioral adaptations to AAF were evaluated in terms of post-feedback slowing (putative larger IOI at keystrokes following AAF), pitch error rate, and distance of pitch errors from AAF (number of keystrokes away from current AAF).

MEG Recording and Pre-processing

Participants were comfortably seated in an electromagnetically shielded room (Vacuumschmelze, Hanau, Germany). Magnetic fields were recorded using a 306-sensor Neuromag Vectorview MEG (Elekta, Helsinki, Finland) with 204 orthogonal planar gradiometers and 102 magnetometers at 102 locations. The head movement was controlled by means of a head-position indicator (HPI) with coils attached to the scalp. Two electrode pairs recorded a bipolar electrooculogram (EOG) to control for horizontal and vertical eye movements - one pair was attached above and below the left eye, the other with two electrodes on the outer canthi. Additionally, a bipolar ECG channel was recorded with electrodes attached to the right clavicle and left ribs.

Signals were sampled at a rate of 1000 Hz with a bandwidth ranging from direct current (DC) to 330 Hz. During the experiment, participants had their right arm resting on a pillow located at a small table. This procedure allowed as comfortable as possible finger movements without inducing arm or shoulder movements that might have influenced the MEG recording.

External interferences in the data were suppressed offline by the signal space separation method (SSS Maxfilter Neuromag; Taulu et al. 2004). This algorithm was further used to transform individual data to a default head position in order to perform statistical analyses across participants in sensor space. The head displacement of participants was < 5mm. Only in one subject with an average head displacement above 5mm (but below 1cm: participant #15) an additional tempo-spatial filtering algorithm was applied to correct for head movements (MC Neuromag; Taulu and Kajola,

2005; Taulu and Simola, 2006). On average the head displacement in all participants was 1.8 (2) mm (range 0.5 – 4 mm; participant #15 excluded in this average).

Subsequent data analyses were performed with Matlab (The MathWorks, Inc., MA, USA) and the FieldTrip toolbox (Oostenveld et al. 2011). The main analysis was conducted using a set of 102 magnetometer sensors, as they are most sensitive to deeper cortical sources (Hansen et al., 2010; Parkkonen et al., 2009). For a complementary analysis conducted with the planar gradiometers see the **Supplementary Material** available online **(Figures S1-S3)**.

The continuous data were filtered offline with a high-pass filter at 1Hz (Linear-phase FIR filter as implemented by Fieldtrip with 'firls' option, two-pass, filter order = 3000). In addition, an independent component analysis-based procedure was used to remove the ocular and electrocardiographic artifacts (FastICA, symmetric approach, hyperbolic tangent – tanh – as nonlinear function; Hyvärinen and Oja, 2000). In order to detect which IC was related to the heartbeat signal, we followed the procedure suggested in the Fieldtrip tutorial (http://www.fieldtriptoolbox.org/example/use_independent_component_analysis_ica_to_remove_ecg_artifacts). In brief, we used both, the time and the frequency data of the ECG to detect the QRS-complex and to compare its profile with similar patterns found in the IC space. We did not use the EOG signal in our IC removal algorithm itself but we visually double-checked that the components we had marked as responsible for eye movements had a similar temporal profile as the ECG signal. For each subject there were between 2-4 independent components (IC) removed. Note that although there are 102 magnetometers, the default SSS Maxfilter settings reduce the dimensionality (rank) of the data to an approximate number of 72. Therefore, around 68-70 ICs

remained after excluding the artifactual components.

Time-frequency representation

The time-frequency representation (TFR) of the signals in the sensor space was performed in trial epochs ranging from -1 to 1 s time-locked to the events of interest: correct keystrokes (i) with normal auditory feedback (NAF), (ii) with alterations of serial order (ASO) feedback, and (iii) with unrelated auditory feedback (UAF) alterations. There were approximately 200 artifact-free data epochs for each AAF condition (ASO, UAF) per participant. Among the larger number of artifact-free data epochs with normal feedback (around 800), we selected a reduced set of 400 data epochs matched as much as possible in timing (IOI) and keystroke velocity to the ASO and UAF trials. Note that large number of trials (200, 400) leads to better signal-to-noise ratio (Gonzalez-Moreno *et al*., 2014) and therefore is likely to facilitate sensitivity of the magnetometers to deep sources (Parkkonen *et al.*, 2009).

The MEG data epochs in the interval [−1,1] s were convolved with complex Morlet wavelet functions to obtain at each sensor and epoch a TFR of the phases and amplitudes of the wavelet-transformed MEG signal x(t). We selected as number of cycles $\eta = 7$. The frequency domain was sampled from 4 to 100 Hz in bins of 1 Hz. This range can be subdivided into the theta (4–7 Hz), alpha (8–13 Hz), beta (14–30 Hz) and gamma (30–100 Hz) frequency bands. Changes in the event-locked spectral power were evaluated by means of the wavelet energy, which is computed as the average across epochs of the squared norm of the response-locked complex wavelet transform. Our main interest was to assess the dynamics of ongoing oscillatory activity, which is

modulated but not evoked or phase-locked by the onset of the stimulus (Lopes da Silva and Pfurtscheller, 1999). Accordingly, we estimated the induced activity by subtracting the evoked oscillatory activity from the total wavelet energy (Herrmann et al., 2004). Next, we normalized the induced spectral power with respect to a baseline interval by subtracting and dividing, for each condition, sensor, frequency and time point separately, the average baseline power in the pre-keystroke interval [-0.2, -0.1] s. The resulting normalized induced spectral power was expressed as percentage of relative power change. This normalization procedure reduced the effects of inter-subject and inter-sensor variability.

Statistical analysis

Behavioral data were analyzed by means of a non-parametric pair-wise permutation test across subjects (Good, 2005) to assess differences between different feedback conditions (ASO – NAF, UAF – NAF, ASO – UAF). The test statistic was the difference in sample means. We performed n = 5000 rearrangements, drawn at random from the complete permutation distribution (Monte Carlo permutation test). The p-values were computed as the ratio of the number of replications of the test statistic having larger absolute values than the experimental difference divided by n. In addition, we report a non-parametric effect size estimator, PS_{dep}, following Grissom and Kim (2012). PS_{dep} is the probability that in a randomly sampled pair of values (one matched pair) the value from Condition B (which for instance has larger values) will be greater than the value from Condition A. The maximum value is PS_{dep} = 1. More details are provided in the Supplementary Material available online. In the case of multiple test statistics being evaluated, we applied an adaptive two-stage

linear step-up procedure (Benjamini et al., 2006) to control the false discovery rate (FDR) at level q=0.05. In those cases, the corrected threshold p-value obtained from the FDR control procedure, termed pth, is provided.

Statistical analysis of the time–frequency data in the sensor space was conducted at the group level using permutation tests with a cluster-based threshold correction to control the family-wise error (FWE) at level 0.05 (dependent samples t-test, 1000 iterations; Maris and Oostenveld 2007). Contrasts of all single conditions (ASO – NAF, UAF – NAF, ASO – UAF) were performed with this approach – always testing the *null hypothesis* of no between-condition difference in the time-frequency representation of the induced oscillatory activity. Experimental cluster-based test statistics being in the 2.5th and 97.5th percentiles of the permutation distribution were considered significant (two-tailed test, $p < 0.025$).

Here the cluster-based non-parametric permutation tests were applied in each contrast to the theta and beta frequency bands and within the time interval from 0.15 to 0.4 s relative to the keystroke events.

Source reconstruction

To localize the sources of the effects obtained in the sensor space, we used a dual procedure combining Common Spatial Pattern (CSP) analysis and dipole fitting (see e.g. Nierula et al., 2013).

The CSP algorithm (Blankertz et al. 2008) is a method used to analyze multi-channel data based on recordings from two conditions. CSP leads to the generalized eigenvalue decomposition of the original signal $x(t) \in \mathbb{R}^C$ into $x_{CSP}(t) \in \mathbb{R}^C$ (see details in the **Supplementary Material**

available online). The decomposition generates C spatial filters (w_j, j = 1, 2,..., C; C being the number of channels) and C spatial patterns (a_j, j = 1, 2,..., C), after applying an optimization criterion, such that CSP filters maximize the variance of the spatially filtered signal for one condition while minimizing it for the other condition. Note that the variance of bandpass-filtered data is equal to the spectral power of the signal in a specific frequency range (Blankertz et al., 2008). Accordingly, CSP is usually applied to bandpass-filtered signals in order to discriminate between conditions characterized by oscillatory activity.

Here, CSP analysis was conducted in the time-frequency ranges of statistical effects obtained in sensor space (see *Statistics*). Similarly to the time-frequency analysis, for the CSP analysis we subtracted the average of evoked responses from the total oscillatory activity (Kalcher and Pfurtscheller, 1995; Nierula et al., 2013.)

Note that in the sensor space the statistical analysis revealed significant between-condition effects, namely *increases* in induced activity (in all contrasts between conditions: ASO – UAF, ASO – NAF, UAF – NAF, see *Results*). Accordingly, the patterns associated with the *three largest* eigenvalues (i.e., being associated with the strongest between-condition increase in induced activity in the time-frequency windows of statistical effects) were subjected to source modeling. The selected set of three CSP patterns was assumed to account for the main between-condition differences (as in Brain-Computer-Interface studies, Blankertz et al., 2008). Significantly, however, the spatial patterns a_j do not represent themselves a *difference* between signals from two conditions but are associated with CSP components, z_j, representing the time course of a corresponding source activity. The CSP components relate to sources maximally different in power

between the conditions. As in Nierula et al., (2013), equivalent dipole modeling was performed on the selected a_j patterns.

For source reconstruction, we performed the following steps:

(i) Individual T1-weighted MRI images (3 T Magnetom Trio, Siemens AG, Germany) were used to construct topographical representations of the cortical surface of each hemisphere with Freesurfer (http://surfer.nmr.mgh.harvard.edu/)

(ii) Co-registration of the MR and MEG coordinate systems was performed with an automated algorithm available in the MNE software (mne_analyze: http://www.martinos.org/mne/stable/index.html) using the HPIs and the digitized points on the head surface (Fastrak Polhemus). In addition, we verified that the three anatomical (fiducial) locations (the nasion and the left and right preauricular points) were correctly co-registered between both coordinate systems and made some minor manual modifications to improve their alignment in 7 out of 20 subjects.

(iii) Forward calculations: With the MNE toolbox we computed boundary element conductivity models (BEM) for each participant and selected the inner skull surface as volume conductor geometry. Then, we created as source space a grid in the MNI space template brain (as used in SPM8) with 4mm resolution and warped this grid into the subject-specific space using individuals' inverse homogenous transformation matrices (obtained during normalization of individual MR images). This step allowed us to have a common grid in MNI coordinates across subjects.

(iv) Inverse calculations: Source reconstruction of the CSP patterns was performed with

equivalent current dipole (ECD) modeling as implemented by FieldTrip, and using one or two dipoles as solution. The 102-sensors montage of the magnetometers and corresponding CSP spatial patterns was selected for this analysis. In the first estimation the optimal location was found by fitting the dipole at each point of the grid with 4mm-resolution. Subsequently, the optimal grid coordinate was used as starting point for a more precise fit using a nonlinear search algorithm. A model with at least 75% of goodness-of-fit (GOF) was accepted for further statistical analysis. The anatomical locations corresponding to each dipole were extracted from the Automated Anatomical Labeling (AAL) digital atlas of the human brain (Tzourio-Mazoyer et al., 2002; here we used 116 labels including bilateral areas and excluding the medulla, midbrain, pons, and cerebellar white matter).

(v) Statistics of inverse calculations: Because we applied CSP and dipole fitting to time-frequency windows of the data showing significant effects in sensor space, the dipole fitting results were not tested against the null hypothesis of no between-condition difference. Rather, we tested the null hypothesis that across subjects the fitted dipoles could be located across all grid positions (in MNI space) with the same probability. Details are provided in the **Supplementary Material** available online. In brief, we assessed the probability of grid points falling within each anatomical location from the AAL atlas, p_{loc}. Our locations of interest were the cingulate gyrus, the temporal gyrus, the cerebellum, the SMA and the functional area of the dorsolateral prefrontal cortex (DLPFC: contributing to the anatomical area of the middle frontal gyrus: labels Frontal_Sup and Frontal_Mid the AAL atlas; Brodmann areas 9 and 46). For each of those locations, we treated the results as a *binomial*

*experiment*t consisting of a fixed number n of statistically independent Bernoulli trials (n = 20 subjects), each with a probability of success p_{loc}, and we counted the number of successes *k* (meaning *k* subjects exhibited that location after dipole fitting; details on the binomial experiment are provided in the **Supplementary Material** available online). We derived the probability that at least *k* subjects out of *n* have a source in the same specific location, P(k,n). The final p-value was corrected for multiple comparisons arising from the five locations of interest by using the Bonferroni correction: $\alpha / 5 = 0.01$, with $\alpha = 0.05$. Accordingly, the null hypothesis was rejected for any of the locations being tested whenever there was at least the minimum number of subjects *k* showing that same specific location, with a probability P(k,n) below the corrected significance threshold 0.01.

Results

Behavioral Data

A scheme listing the abbreviations corresponding to each control and experimental conditions is displayed in **Figure 1**. Data are provided as mean and, in parentheses, standard error of the mean (SEM). In this section, we report results for the main performance block. Behavioral results for the previous familiarization (training) block can be found in the Supplementary Material available online. In brief, across the three training trials participants demonstrated rapid improvements in performance as reflected in faster average tempo and reduced temporal variability.

Performance block: Across all trials and for each sequence type participants played on average 671(6) keystrokes. In trials with modified feedback, the rate of AAF was one in every 8.37(0.05) keystrokes or every 3140(130) ms. On average the keystroke velocity in normal trials was 56(1),

which was significantly smaller than the value in each of the conditions with modified feedback ($p < pth = 0.01$; 57 [1] both in ASO and UAF trials, $PS_{dep} = 0.80$ and 0.70, respectively. These trials did not differ in keystroke velocity). Accordingly, modified auditory feedback induced a larger keystroke velocity, as previously reported (Furuya and Soechting, 2010).

_____ Figure 2 around here _____

Error rates. The main outcome was that in trials with ASO feedback, but not in trials with UAF feedback, there was a larger rate of self-produced pitch errors as compared with the rate in normal trials (mean 0.025 [0.003] in ASO and 0.019 [0.003] in NAF trials, $p < pth = 0.01$, $PS_{dep} = 0.80$; mean 0.023 [0.003] in UAF trials, $p > 0.05$; **Figure 2A**). The error rates in trials with ASO and UAF were not significantly different. The pitch error rate increased across trials with ASO (from an initial average rate of 0.021 [0.004] to 0.034 [0.004], $p < pth = 0.007$, $PS_{dep} = 0.75$), whereas it remained stable across trials with UAF and trials with normal feedback ($p > 0.05$ in both cases). In addition, the percentage of ASO events inducing pitch errors was 0.25 (0.02), significantly larger than the percentage of UAF events triggering errors, which was 0.19 (0.02; $p = 0.024$, $PS_{dep} = 0.75$). The pitch value and ordinal position of the errors induced by AAF events were consistent with compensatory changes in the next rendition of the sequence, most prominently in ASO trials (See further details in the **Supplementary Material** and **Figure S4** available online). The ASO-induced compensatory changes reflected alterations in the sequential organization of the events planned for production.

Finally, assessment of the questionnaires filled out by the participants revealed that they overestimated the number of pitch errors due to the presence of AAF, an outcome that has been

reported in a previous behavioral study (Pfordresher and Beasley, 2014). The subjective number estimate of self-produced errors per sequence type was 19 (1), whereas the number of self-produced errors was 15 (2), and the difference was significant ($p = 0.016$, $PS_{dep} = 0.80$). Of note, more participants reported recognizing the occasional presence of AAF unrelated to the sequence content than noticing AAF of the ASO kind (16 and 13 participants, respectively, see **Supplementary Material** available online).

Timing. On average, participants played at a rate of 1 keystroke every 384 [10] ms in trials without AAF. No significant changes between auditory feedback conditions were found in the average IOI. However, the temporal variability (CV) was significantly larger in trials with each kind of AAF compared to normal trials ($p < pth = 0.022$ in both comparisons, $PS_{dep} = 0.70$ for ASO relative to NAF and $PS_{dep} = 0.80$ for UAF relative to NAF). Accordingly, both kinds of AAF induced a poorer performance within the trial with regard to variability in timing.

AAF induced alterations in the timing of the subsequent keystrokes. UAF induced a significant post-feedback slowing in the next (+1) and subsequent (+2) keystroke, as reflected in the significantly larger mean IOI at those positions relative to UAF alterations (393 [10] ms at the postUAF keystroke; 391 [10] at the post2UAF keystroke; in both cases the mean IOI was significantly larger than the mean IOI at UAF events 383 [9] ms; $p < pth = 0.018$, $PS_{dep} = 0.75$ and 0.8, respectively; **Figure 2B**). ASO feedback did not lead to changes in timing in the immediately subsequent keystroke (388 [10] ms at +1 and 385 [10] ms; $p > 0.05$), but it did induce significant post-feedback slowing at +2 keystrokes from the feedback alteration (391 [10] ms, $p < pth = 0.018$, $PS_{dep} = 0.75$). Furthermore, a control analysis comparing the mean IOI in trials with normal auditory

feedback and in keystrokes subject to either UAF or ASO feedback did not reveal any significant result ($p > 0.05$), supporting that changes in timing were evident only in the keystrokes *following* AAF.

We then assessed the general changes in performance due to training: Across trials with normal auditory feedback (trial 1 vs 11) there was no change in average tempo, but there was a significant increase in the extent of temporal variability (CV 0.24 [0.02] trial 1 and 0.31 [0.03] trial 11, $p < pth = 0.0028$, $PS_{dep} = 0.80$). This outcome indicated that temporal accuracy in normal trials decreased throughout training, possibly due to the interspersed trials with AAF.

Time-frequency analysis in the sensor space

The effects of the alterations of auditory feedback on oscillatory power in the sensor-space are displayed in **Figure 3.** The cluster-based permutation test, which was performed in the latency range from 150 ms to 400 ms post-keystroke, revealed a significant positive difference between the theta-band oscillatory activity induced by the feedback-based ASO and the normal auditory feedback ($p< 0.025$, two-sided test). In this latency range, the difference reflected an enhanced theta-band spectral power most pronounced over *midline frontoparietal* sensors (**Figure 3,** left panel). No significant differences between these conditions were found in the beta band.

The effect of UAF, when compared to the effect of normal auditory feedback, was also a significant increase in the theta-band oscillatory activity and from 150 ms to 400ms post-keystroke ($p < 0.025$). In this time window, the difference was observed as an enhanced theta-band spectral power induced by the UAF and most pronounced over *right frontoparietal sensors* (**Figure 3**,

middle panel). The between-condition differences in the beta band were non-significant.

A final planned comparison between both types of AAF (ASO – UAF) in the same latency range 150 – 400 ms revealed a significant difference in the beta ($p < 0.025$), but not in the theta band ($p > 0.05$), due to increased beta-band oscillatory activity over *frontal* sensors (positive cluster; **Figure 3**, right panel).

_____ Figure 3 around here _____

Common spatial patterns and source localization

The statistical within-group effects reported at the sensor level in previous section showed enhanced oscillatory activity in one feedback condition relative to the other (ASO – NAF, UAF – NAF, ASO – UAF). Accordingly, we selected the CSP patterns corresponding to the *three largest* eigenvalues, which were associated across subjects with a monopolar or dipolar pattern. **Figure 4** shows three theta-band CSP patterns from two representative subjects for the ASO – NAF comparison. Similarly, **Figure 5** shows two theta-band CSP patterns from the same representative subjects for the UAF – NAF comparison. The specific comparison between modified feedback conditions, ASO-UAF, is represented by the beta-band CSP patterns in **Figure 6**.

Source reconstruction of the beta and theta-band CSP patterns was subsequently performed at the single-subject level with equivalent dipole modeling. Depending on the CSP pattern topography, we fitted one or two dipoles. The resulting GOF of the models was in the range 77-86% (median = 83%).

The equivalent current dipole algorithm revealed different anatomical locations as main

generators of the effects found at the sensor level. Under the null hypothesis of a uniformly distributed localization of each source across the whole brain, we here exclusively report significant results of source localization based on the finding of the same anatomical source in at least k out of 20 subjects and with a p-value P(k,n) below the corrected significance threshold 0.01. The probability P(k,n) and the minimum number of k successes (min_k) are provided below.

_____ Figure 4 around here _____

_____ Figure 5 around here _____

Coordinates of the sources are given as median and median absolute dispersion (MAD) across subjects. For the ASO – NAF feedback comparison (**Figure 4D-F**), the sources of enhanced theta-band activity were located to the cingulate gyrus (14/20 subjects, coordinates of the locus of activity in the MNI space are X = 0 -36 28 [3 4 12] mm in the posterior cingulate gyrus (left, L); min_k = 7, P(14,20) = 7 x 10^{-10}), bilaterally to the cerebellum (13/20 subjects, coordinates of the locus of activity X = 26 -56 -34 [8 5 10] mm and X = -22 -52 -24 [7 3 7] mm in lobule VI [right, R; L]; min_k = 12; P(13,20) = 0.0026) and also bilaterally to the middle temporal gyrus (14/20 subjects, coordinates of the locus of activity X = 52 -38 -6 [7 18 8] mm and -52-28 -4 [3 13 5] mm; min_k = 13; P(14,20) = 0.0010).

In the case of the UAF – NAF feedback comparison (**Figure 5C-D**), the sources of increased theta-band activity were located to the cerebellum (13/20 subjects, coordinates of the locus of activity X = 4 -48 -42 [12 5 9] mm in the posterior lobe, lobule IX (R); min_k = 12, P(13,20) = 0.0026), and the bilateral inferior temporal gyrus (15/20 subjects, coordinates of the locus of activity X = -50 -34 -20 [5 11 6] mm and 52 -3 -16 [5 10 4] mm; min_k = 13; P(15,20) = 2 x 10^{-4}).

Finally, the effect of enhanced beta-band oscillatory activity obtained for the specific comparison between ASO and UAF trials was localized (see **Figure 6C-D**) to the cingulate gyrus (15/20 subjects, coordinates of the locus of activity X = 2 -36 32 [8 8 4] mm in the posterior cingulate gyrus (L); min_k = 7, P(15,20) = 3 x 10^{-11}) and the cerebellum (14/20 subjects, coordinates of the locus of activity X = 16 -58 -26 [14 8 12] mm in the posterior lobe, lobule VI (R); min_k = 13; P(14,20) = 6 x 10^{-4}).

Additional sources found for each comparison in a smaller number of participants (5-9) are reported in detail in the Supplementary Material, yet these effects were non-significant according to our statistical analysis at the group level.

As a control analysis, we computed the power spectral density (PSD, in fT^2/Hz) of the magnetometers during playing in performance blocks. Muscle-artifacts have been shown to induce oscillatory activity that overlaps with neural activity in the higher (> 20Hz) frequency range (Muthukumaraswamy, 2013). This could affect the localization of high frequency activity in structures such as the cerebellum or temporal cortices. Our PSD analysis, however, revealed that during performance, compared to rest periods in-between performance trials, there was no general increase of PSD in the higher frequency range but rather a general attenuation of PSD **(Figures S5 and S6**). Accordingly, the changes in beta oscillations reported in our study are restricted to changes in the event-locked induced activity and do not reflect general power changes influenced by muscle-artifacts. This strongly supports that the cerebellar sources reported in this study are most likely related to the specific processing of the type of event (i.e. UAF or ASO relative to NAF or ASO relative to UAF). In addition, it should be noted that the cerebellum, which was one of the

main sources found in 14/20 participants to be related to processing modified feedback that interferes with serial order via modulation of beta oscillations (ASO-UAF comparison), was also a source in the majority of the remaining participants when considering the CSP associated with the lower eigenvalues (4 to 10 additional subjects). This, however, also means that these additional CSP were less discriminative of the between-conditions difference in beta power. We have therefore aligned with the common practise and limited our statistical analysis at the group level to the most discriminative CSP corresponding to the three eigenvectors at the beginning of the eigenvalue spectrum (Blankertz et al., 2008).

Finally, source modeling performed separately in the planar gradiometers confirmed the majority of these sources, albeit with a larger inter-individual variability (i.e. with the sources of interest being located in fewer subjects: **Supplementary Figures S2** and **S3**).

These results therefore highlight that the sources of oscillatory activity underlying processing of each kind of AAF during performance can be dissociated both in space and spectral content.

_____ Figure 6 around here _____

Correlation analysis

The relation between oscillatory source activity and behavioral parameters was assessed with the non-parametric Spearman ρ. The pairs of variables used for the correlation analyses were selected based on the source localization and behavioral results. For instance, the magnitude of the dipole moment (in nAm) associated with the CSP pattern leading to differential source activity in epochs

with ASO feedback and UAF feedback (ASO – UAF difference) was correlated with differences in pitch error rates and differences in post-feedback slowing. Note that, for this analysis, the time course of the signals was normalized for each subject to a standard deviation of 1, in order to have a similar scale in the CSP patterns (which otherwise have arbitrary scales). Therefore, the magnitude of the dipole moments (in nAm) was estimated in CSP patterns of comparable magnitude across subjects.

The p-values were corrected for multiple comparisons using the control of the FDR at level q = 0.05 previously described (*Statistics*). We found that the magnitude of the dipole moment the cingulate cortex corresponding with the ASO – UAF difference pattern in beta-band oscillatory activity significantly correlated with the difference in error rates ($\rho = 0.731$, p-value = 0.002< pth = 0.0235; N = 15; **Figure 7**). Thus, larger cingulate beta-band activity was induced by ASO relative to UAF in participants who had larger pitch error rates in those trials. No significant correlations were found for any other source of activity in ASO or UAF epochs relative to NAF epochs.

_____ Figure 7 around here _____

Discussion

We have shown that the oscillatory sources underlying the processing of different kinds of alterations of auditory feedback during sensorimotor learning can be dissociated in both their spatial and spectral content. Specifically, processing UAF or ASO feedback relative to normal feedback induced theta-band oscillations in the cerebellum and superior temporal gyrus.

Processing ASO feedback relative to normal feedback additionally engaged the cingulate gyrus. A planned post-hoc comparison between the ASO and UAF experimental conditions revealed that beta-band oscillatory activity in the cingulate cortex and cerebellum is enhanced by processing ASO. Furthermore, we also found a dissociation of the effect of each kind of AAF on behavioral performance during training, with exclusively ASO leading to larger pitch error rates when compared with normal feedback. Taken together these results suggest that dedicated neural mechanisms monitor the correspondence between the sources of auditory and motor information on the serial order of the produced actions during the initial phase of sequence learning, thereby contributing to updating the sensorimotor representations.

Theta oscillations reflect the general processing of alterations of auditory feedback

Our participants demonstrated behavioral adjustments in the keystrokes subsequent to the events with modified auditory feedback. The adjustments were reflected in the post-feedback slowing at the keystroke following UAF and at two keystrokes following UAF or ASO. Significantly, the slowing of responses following false external feedback, as used in our task, resembles the slowing after self-produced errors (Saunders and Jentzsch, 2012). Our data thus suggest that the oscillatory responses following each kind of AAF might partly reflect cognitive control processes that detect unexpected feedback (a potential error) and implement an increase in response caution in the subsequent keystrokes (Dutilh et al. 2012).

Previous studies investigating neuronal processing of incorrect feedback, using different paradigms ranging from motor behavior to gambling tasks, have consistently revealed an

involvement of the mid-frontal areas, including the ACC (for a recent review see Luft 2014; see also Ridderinkhof et al. 2004). Theta oscillations in the medial frontal cortex as well as theta frequency coupling between mid-frontal areas, sensorimotor and lateral prefrontal areas are modulated by feedback processing and subsequent behavioral adjustments, often in the form of post-feedback slowing (Cohen et al., 2011, Cavanagh et al., 2009, 2010). Our finding of enhanced frontal theta oscillations following the processing of ASO feedback is in agreement with the interpretation that increased mid-frontal theta oscillations index the detection of a mismatch between the predicted and actual sensory consequences of the action (HajiHosseini and Holroyd, 2013). Interestingly, the larger amplitude of theta oscillations induced by ASO events partially originated in the posterior cingulate gyrus (PCC, median across subjects), which apparently contrasts with the evidence from studies primarily linking the ACC to error-monitoring (Holroyd and Coles, 2002; Ridderinkhof et al. 2004). Note, however, that the PCC is also a key region in action- and error-monitoring (Agam et al, 2011; Heilbronner and Platt, 2013) and might be particularly relevant when error agency is modulated (de Bruijn et al. 2009). Significantly, UAF events did not induce enhanced theta oscillations in cingulate regions as measured by the magnetometers (but see the **Supplementary Material** available online). This suggests that AAF related to the sequence content (ASO) might have been processed as more salient by the cingulate cortex, despite the UAF events potentially being associated with a larger sensory distance from the target pitch.

An interesting aspect to consider in future studies is the investigation of the event-related fields and their modulation by the different types of AAF. Random pitch alterations during piano performance elicit a frontocentral negative-going event-related potential (ERP) peaking at 250ms,

termed feedback-error related negativity (fERN or FRN), and generated by the anterior cingulate cortex (Maidhof et al., 2015). Because the main oscillatory content of the FRN lies in the theta frequency range (Cohen et al., 2007), future studies should look into its sensitivity to changes in the type of AAF.

The contribution of the temporal lobe to the enhanced theta oscillations during the processing of either kind of AAF relative to normal feedback is in agreement with previous studies. Specifically, the involvement of the auditory cortex in processing salient auditory feedback that mismatches with the predicted outcome has been identified in tasks using regular sequences of sounds (mismatch negativity studies: e.g. Rinne et al. 2000), during singing (fixed shift in pitch: Zarate and Zatorre, 2008; see also recent review by Zarate 2013) or speech (fixed shift in pitch: Chang et al. 2013; Tourville et al. 2008). Importantly, despite the UAF events potentially being processed as more salient auditory events, there were no significant UAF-ASO differences being localized to the auditory cortices. This supports that differences in the sensory distance between the target and actual auditory feedback cannot account for the findings in our study.

With respect to the cerebellum, convergent evidence indicates that this structure computes sensory-prediction error signals which effectively distinguish between the sensory consequences of self-generated and externally produced actions (Brooks and Cullen, 2013; Cullen, 2012). The cerebellum is thus crucial for error-based learning (Diedrichsen, 2005; Wolpert et al., 2001), particularly during the initial stages of motor skill acquisition (Doyon et al., 2003; Lehéricy et al., 2004). The results thus support that theta oscillations induced in the cerebellum after ASO and UAF events indicate the detection of *generic* deviations in the sensory consequences of the

produced actions (see next section for a more specific involvement of cerebellar beta activity in processing ASO).

Changes in beta oscillations during processing feedback-based alterations of the serial order

Pitch error rates increased across time in trials with ASO feedback. In addition, ASO feedback induced larger within-trial error rates than normal feedback, with errors typically occurring in the next rendition of the sequence. This outcome supports that ASO feedback did interfere with the sensorimotor representation of the sequence being performed, thereby leading to the selection of the wrong sequence elements (i.e., incorrect pitch errors) in the next rendition of the sequence. Notably, the pattern of pitch errors induced by ASO was consistent with compensatory changes reflecting alterations in the sequential organization of the events planned for production (similar to Pfordrescher and Palmer, 2006). This specific effect of ASO feedback on (wrongly) updating sequential behavior might be explained by the fact that ASO feedback – but not UAF feedback – simulated a serial-order error that activated the wrong ordinal position during the sensorimotor learning process. The processing of incorrect auditory feedback in this case did influence learning and production of the sequence elements, possibly reflecting a rapid compensation to feedback errors – as reported for speech production or singing (Kort et al. 2014; Zarate and Zatorre, 2008). Support for our interpretation comes from animal studies of vocal learning which show that exclusively when the shifted pitch falls within the pitch content of the sensorimotor sequence (song) – regardless of the absolute error magnitude – AAF elicit compensatory changes and influence

learning (Kelly and Sober, 2014; Sober and Brainard, 2012). By contrast, AAF that fall outside of the history of pitch production are discarded as unreliable (Sober and Brainard, 2012).

The crucial finding in our study was that alterations of auditory feedback of the ASO kind induced an increase in the power of beta-band oscillations across cingulate (median coordinates in the PCC) and cerebellar regions. In addition, larger cingulate beta-band activity in ASO relative to UAF correlated with larger pitch error rates. The cingulate cortex – mainly its anterior portion ACC, but also its posterior portion (PCC) – has been consistently associated with action- and error-monitoring (Holroyd and Coles, 2002; Agam et al, 2011; Heilbronner and Platt, 2013). Specifically, cingulate regions are involved in the selection of appropriate responses to new situations based on the evaluation of reward expectation and reward prediction errors (Carter et al., 1998, Rushworth and Behrens, 2008; Amiez et al., 2012). In other words, the cingulate cortex integrates feedback-related information to update action selection (Rushworth and Behrens, 2008). Accordingly, our working hypothesis is that the increase in cingulate beta oscillations might partly reflect that the result of performance monitoring processes by the cingulate cortex contributes to the integration of the altered auditory feedback into the ongoing sequential learning process and updating the motor plan.

Evidence for a specific involvement of beta oscillations during action evaluation based on feedback remains sparse and inconclusive. Some studies focusing on feedback-based response learning have maintained that beta power increases exclusively following positive feedback (Cohen et al., 2007, 2011), whereas others also found an increase in beta power after negative feedback (Koelewijn et al. 2007). More recently, in a reward-learning task, it has been demonstrated that beta

oscillations in the dorsolateral prefrontal cortex (DLPFC) mediate reward learning and working memory (HajiHosseini and Holroyd, 2015). Because the DLPFC is anatomically and functionally associated with the ACC and the PCC (Parvizi et al. 2006; Petrides and Pandya, 1999; Vogt and Pandya, 1987), and these regions are engaged in monitoring the serial order of short sequences of stimuli in working memory (Amiez at al; 2007; Petrides, 1991), it is plausible that beta oscillations across cingulate and dorsolateral prefrontal regions facilitate updating the representation of the order of actions in a sequence based on feedback-processing. Our dipole fitting procedure did not, however, point to the prefrontal cortex as one of the sources of beta oscillatory activity (see methodological considerations).

An alternative interpretation is that the higher level of beta power following keystrokes with ASO feedback reflects the *suppression* of the prepared upcoming sequential actions or an estimation of the likelihood of the need for a novel voluntary action, as reported for sensorimotor beta oscillations (Jenkinson and Brown, 2014; Swann et al 2009, Zhang et al 2008). However, because we found enhanced beta oscillations outside of the sensorimotor areas within the cortico-basal ganglia-thalamocortical circuits (such as the SMA, one of our regions of interest), our data favor rather the prior interpretation that they play a role in updating the ongoing sensorimotor representation of the sequence elements based on feedback-processing.

The cerebellum, in addition to contributing to the functions mentioned above, contributes to extracting sequential order information from incoming sensory information (Molinari et al., 1997; Restuccia et al. 2007). Additional evidence stemming from an MEG study supports that 25-35Hz oscillations in the cerebellum are enhanced after violations of predicted somatosensory feedback

(Tesche and Karhu, 2000). These findings therefore support the idea that the cerebellum might be involved in processing violations of auditory (sensory) feedback during sequence learning. Accordingly, they are consistent with the effect of larger cerebellar beta activity for ASO trials as compared with UAF trials, which possibly reflects an incorrect update of the mapped sensorimotor representations thereby leading to larger error rates in ASO trials. Our interpretation, however, necessitates future studies using AAF of different kinds, including serial shifts in pitch, in order to investigate further the relation between cerebellar activity, beta oscillations and the different kinds of AAF.

Methodological considerations

Our approach aimed at detecting spatial specificity in the locations of the source of neuronal oscillations associated with each between-condition difference revealed at group level in the sensor space. To this aim, we used CSP patterns with the largest eigenvalues – reflecting the largest ratio of between-condition spectral power – to perform source localization with equivalent current dipole modeling.

Of note, the locations of the sources revealed with ECD modeling have limited accuracy as determined by the spatial accuracy of MEG (Hansen et al., 2010; Hari et al., 1988). The results, therefore, need to be interpreted with caution. Importantly, however, the brain areas in which the dipoles were localized are in line with previous fMRI evidence (Pfordresher *et al*., 2014) and were in our study independently confirmed by the separate analysis of the signals from planar gradiometers (**Supplementary Material** available online). One inconsistency with previous findings

supporting the involvement of the ACC in action-monitoring (Carter et al., 1998; Holroyd and Coles, 2002) was the localization of sources in the posterior part of the cingulate gyrus (median across subjects). The limitations that affect source localization of MEG data (Hansen et al., 2010; Hari et al., 1988) might account for this apparent discrepancy. There is, however, growing evidence that cingulate regions posterior to the ACC – the PCC – also have a crucial role during error-monitoring (Agam et al, 2011; Heilbronner and Platt, 2013) and are affected by error agency (de Bruijn et al. 2009).

Our findings complement a growing body of evidence stemming from MEG studies in support for the sensitivity of MEG sensors to deeper structures, such as the cerebellum or the cingulum (Bourguignon et al., 2013; Martin et al., 2006). An advantage of recent studies might be the focus on the analysis of oscillations, in particular, high frequency oscillations (above 30Hz), which facilitates the localization of sources in the cerebellum (E/MEG: Dalal et al., 2008; Dalal et al., 2013). Indeed, recent MEG studies support an involvement of cerebellar activity in functions as diverse as movement generation (Bourguignon et al., 2013; Gross et al., 2002; Jerbi et al., 2007; Pollok et al., 2005), timing and rhythm (Fujioka et al., 2012; Martin et al., 2006) or somatosensory processing (Tesche and Karhu, 1997, 2000).

Crucially, however, muscle-artifacts have been shown to induce oscillatory activity that overlaps with neural activity in the higher (>20Hz) frequency range (Muthukumaraswamy, 2013). This could affect the localisation of high frequency activity in structures such as the cerebellum or temporal cortices. Here we addressed this issue by (i) assessing the power spectral density of the MEG recordings during performance relative to rest and finding no enhanced level of PSD above

20Hz, but rather a significant attenuation during performance of alpha and beta PSD; and (ii) by focusing the analysis of source localization on event-related changes in induced oscillatory activity. Each event of interest (NAF, ASO, UAF) in our experiment was locked to a key press or movement that was similar across conditions, with only the auditory feedback being modified in the different conditions. Potential muscle-artifacts associated with key presses should thus be similar across conditions as well.

Accordingly, we consider that muscle-artifacts are not likely to account for the result of the cerebellum being the source of larger beta oscillatory activity in the ASO relative to the UAF condition.

Finally, it should be noted that in our study no activation was localized to the SMA, an area which has been previously linked to the encoding of sequential actions (Tanji and Shima, 1994; Gerloff et al., 1997; Clower and Alexander, 1998; Wiestler and Diedrichsen, 2013). A potential explanation is that in the current study we investigated the sources of oscillatory activity induced by the mismatch of auditory feedback. Processing AAF during sequence learning was primarily reflected in the cingulate cortex and the cerebellum (to a different degree depending on the ASO and UAF trials). Moreover, in a few participants (between 5-9, non-significant effects at the group level) we found activation associated with processing the different types of AAF in other regions such as the primary motor and sensorimotor cortices, or the dorsolateral and medial prefrontal cortices – regions also relevant during sequence encoding (Wiestler and Diedrichsen, 2013), yet not in the SMA. Consequently, although the SMA might be crucial for the encoding of sequential movements, our results overall indicate that this region may not respond to violations of auditory

information that do not correspond to the sequential action.

Conclusion

These findings reveal a novel role for beta oscillations in tracking serial order during initial sensorimotor learning and in updating the sensorimotor mapping of sequential elements. To our knowledge, the findings are novel in the music performance, speech production and singing literature, yet they can significantly contribute to the understanding of sensorimotor learning in all these types of behavior.

Our results also have implications for research on movement disorders, such as dystonia or Parkinson's disease (PD). Cerebellar activity and its connectivity to cortical areas is crucially involved in generating the motor symptoms in these disorders (Rascol et al., 1997; Neumann et al., 2015). In addition, patients with PD or dystonia exhibit anomalous sequence learning skills (Carbon et al., 2008; 2010; Herrojo Ruiz et al., 2014b). Accordingly, future research comparing cerebellar beta oscillations during sensorimotor sequence learning in healthy and disease populations could help further elucidate oscillatory mechanisms influencing the integration of sequential motor and auditory information during skill acquisition.

Acknowledgements

We thank Yvonne Wolff for her invaluable help with the MEG data acquisition and Carsten Allefeld for engaging in fruitful discussions. We also thank Mark Bangert for providing crucial information on the MEG-compatible keyboard. This research is supported by the German Research Foundation (DFG) through project HE 6013/1-2 to MHR. VN acknowledges support from the Russian

Academic Excellence Project ‘5–100’.

References

Agam Y, Hämäläinen MS, Lee AK, Dyckman KA, Friedman JS, Isom M, Makris N, Manoach DS (2011): Multimodal neuroimaging dissociates hemodynamic and electrophysiological correlates of error processing. Proceedings of the National Academy of Sciences.108(42):17556-61.

Amiez C, Petrides M (2007): Selective involvement of the mid-dorsolateral prefrontal cortex in the coding of the serial order of visual stimuli in working memory. Proceedings of the National Academy of Sciences. 104(34):13786-91.

Amiez C, Sallet J, Procyk E, Petrides M (2012): Modulation of feedback related activity in the rostral anterior cingulate cortex during trial and error exploration. Neuroimage. 63(3):1078-90.

Averbeck BB, Chafee MV, Crowe DA, Georgopoulos AP (2002): Parallel processing of serial movements in prefrontal cortex. Proceedings of the National Academy of Sciences. 99(20):13172-7.

Bangert M, Peschel T, Schlaug G, Rotte M, Drescher D, Hinrichs H, Heinze HJ, Altenmüller E (2006): Shared networks for auditory and motor processing in professional pianists: evidence from fMRI conjunction. Neuroimage. 30(3):917-26.

Bartolo R, Prado L, Merchant H (2014): Information processing in the primate basal ganglia during sensory-guided and internally driven rhythmic tapping. The Journal of Neuroscience. 34(11):3910-23.

Benjamini Y, Krieger AM, Yekutieli D (2006): Adaptive linear step-up procedures that control the false discovery rate. Biometrika. 93(3):491-507.

Blankertz B, Tomioka R, Lemm S, Kawanabe M, Muller KR (2008): Optimizing spatial filters for robust EEG single-trial analysis. Signal Processing Magazine, IEEE. 25(1):41-56.

Bourguignon M, De Tiege X, de Beeck MO, Van Bogaert P, Goldman S, Jousmaki V, et al (2012):

Primary motor cortex and cerebellum are coupled with the kinematics of observed hand movements. Neuroimage . 66c: 500–7.

Brooks JX, Cullen KE (2013): The primate cerebellum selectively encodes unexpected self-motion. Current Biology. 23(11):947-55.

Carter CS, Braver TS, Barch DM, Botvinick MM, Noll D, Cohen JD. (1998): Anterior cingulate cortex, error detection, and the online monitoring of performance. Science. 280(5364):747-9.

Carbon M, Ghilardi MF, Argyelan M, Dhawan V, Bressman SB, Eidelberg D (2008): Increased cerebellar activation during sequence learning in DYT1 carriers: an equiperformance study. Brain. 131(1):146-54.

Carbon M, Reetz K, Ghilardi MF, Dhawan V, Eidelberg D. Early Parkinson's disease: longitudinal changes in brain activity during sequence learning (2010): Neurobiology of disease. 37(2):455-60.

Cavanagh JF, Cohen MX, Allen JJ (2009): Prelude to and resolution of an error: EEG phase synchrony reveals cognitive control dynamics during action monitoring. The Journal of Neuroscience. 29(1):98-105.

Cavanagh JF, Figueroa CM, Cohen MX, Frank MJ (2011): Frontal theta reflects uncertainty and unexpectedness during exploration and exploitation. Cerebral cortex. bhr332.

Cavanagh JF, Frank MJ, Klein TJ, Allen JJ (2010): Frontal theta links prediction errors to behavioral adaptation in reinforcement learning. Neuroimage. 49(4):3198-209.

Chang EF, Niziolek CA, Knight RT, Nagarajan SS, Houde JF (2013): Human cortical sensorimotor network underlying feedback control of vocal pitch. Proceedings of the National Academy of Sciences. 110(7):2653-8.

Clower WT, Alexander GE (1998): Movement sequence-related activity reflecting numerical order of components in supplementary and presupplementary motor areas. Journal of neurophysiology. 80(3):1562-6.

Cohen MX (2011): Error-related medial frontal theta activity predicts cingulate-related structural

connectivity. Neuroimage. 55(3):1373-83.

Cohen MX, Elger CE, Ranganath C (2007): Reward expectation modulates feedback-related negativity and EEG spectra. Neuroimage. 35(2):968-78.

Cullen KE (2012): The vestibular system: multimodal integration and encoding of self-motion for motor control. Trends in neurosciences. 35(3):185-96.

Dalal SS, Guggisberg AG, Edwards E, Sekihara K, Findlay AM, Canolty RT, Berger MS, Knight RT, Barbaro NM, Kirsch HE, Nagarajan SS (2008): Five-dimensional neuroimaging: localization of the time–frequency dynamics of cortical activity. Neuroimage. 40(4):1686-700.

Dalal SS, Osipova D, Bertrand O, Jerbi K. Oscillatory activity of the human cerebellum: the intracranial electrocerebellogram revisited (2013): Neuroscience & Biobehavioral Reviews. 37(4):585-93.

Dayan E, Cohen LG (2011): Neuroplasticity subserving motor skill learning. Neuron. 72(3):443-54.

de Bruijn ER, de Lange FP, von Cramon DY, Ullsperger M (2009): When errors are rewarding. The Journal of Neuroscience. 29(39):12183-6.

Dehaene S, Meyniel F, Wacongne C, Wang L and Pallier C (2015): The Neural Representation of Sequences: From Transition Probabilities to Algebraic Patterns and Linguistic Trees. Neuron. 88(1): 2-19.

Diedrichsen J, Hashambhoy Y, Rane T, Shadmehr R (2005):Neural correlates of reach errors. The Journal of Neuroscience. 25(43):9919-31.

Doyon J, Penhune V, Ungerleider LG (2003):Distinct contribution of the cortico-striatal and cortico-cerebellar systems to motor skill learning. Neuropsychologia. 41(3):252-62.

Dutilh G, Vandekerckhove J, Forstmann BU, Keuleers E, Brysbaert M, Wagenmakers EJ (2012): Testing theories of post-error slowing. Attention, Perception, & Psychophysics. 74(2):454-65.

Fujioka T, Trainor LJ, Large EW, Ross B. Internalized timing of isochronous sounds is represented in neuromagnetic beta oscillations (2012): The Journal of Neuroscience. 32(5):1791-802.

Furuya S, Soechting JF (2010): Role of auditory feedback in the control of successive keystrokes

during piano playing. Experimental brain research. 204(2):223-37.

Gerloff C, Corwell B, Chen R, Hallett M, Cohen LG (1997): Stimulation over the human supplementary motor area interferes with the organization of future elements in complex motor sequences. Brain 120:1587–1602.

Gonzalez-Moreno A, Aurtenetxe S, Lopez-Garcia ME, del Pozo F, Maestu F, Nevado A (2014): Signal-to-noise ratio of the MEG signal after preprocessing. Journal of neuroscience methods. 222:56-61.

Good P (2005): Permutation Parametric and Bootstrap Tests of Hypotheses. 2nd ed. Berlin: Springer.

Grissom RJ, Kim JJ (2012): Effect sizes for research: Univariate and multivariate applications. 2nd ed. New York: Taylor & Francis.

Groß J, Timmermann L, Kujala J, Dirks M, Schmitz F, Salmelin R, Schnitzler A. The neural basis of intermittent motor control in humans (2002): Proceedings of the National Academy of Sciences. 99(4):2299-302.

Hajihosseini A, Holroyd CB (2013): Frontal midline theta and N200 amplitude reflect complementary information about expectancy and outcome evaluation. Psychophysiology. 50(6):550-62.

HajiHosseini A, Holroyd CB (2015): Sensitivity of frontal beta oscillations to reward valence but not probability. Neuroscience letters. 602:99-103.

Hämäläinen M, Hari R, Ilmoniemi RJ, Knuutila J, Lounasmaa OV (1993): Magnetoencephalography—theory, instrumentation, and applications to noninvasive studies of the working human brain. Reviews of modern Physics. 65(2):413.

Hansen P, Kringelbach M, Salmelin R, editors (2010): MEG: an introduction to methods. Oxford: Oxford university press.

Hari R, Joutsiniemi SL, Sarvas J (1988): Spatial resolution of neuromagnetic records: theoretical calculations in a spherical model. Electroencephalography and Clinical Neurophysiology/Evoked Potentials Section. 71(1):64-72.

Heilbronner SR, Platt ML (2013): Causal evidence of performance monitoring by neurons in posterior cingulate cortex during learning. Neuron. 80(6):1384-91.

Herrmann CS, Munk MH, Engel AK (2004): Cognitive functions of gamma-band activity: memory match and utilization. Trends in cognitive sciences. 8(8):347-55.

Herrojo Ruiz M, Brücke C, Nikulin VV, Schneider GH, Kühn AA (2014a): Beta-band amplitude oscillations in the human internal globus pallidus support the encoding of sequence boundaries during initial sensorimotor sequence learning. Neuroimage. 85:779-93.

Herrojo Ruiz M, Jabusch HC, Altenmüller E (2009): Detecting wrong notes in advance: neuronal correlates of error monitoring in pianists. Cerebral Cortex. 19(11):2625-39.

Herrojo Ruiz M, Rusconi M, Brücke C, Haynes JD, Schönecker T, Kühn AA (2014b): Encoding of sequence boundaries in the subthalamic nucleus of patients with Parkinson's disease. Brain. awu191.

Herrojo Ruiz M, Strübing F, Jabusch HC, Altenmüller E (2011): EEG oscillatory patterns are associated with error prediction during music performance and are altered in musician's dystonia. Neuroimage. 55(4):1791-803.

Holroyd CB, Coles MG (2002): The neural basis of human error processing: reinforcement learning, dopamine, and the error-related negativity. Psychological review. 109(4):679.

Hyvärinen A, Oja E (2000): Independent component analysis: algorithms and applications. Neural networks. 13(4):411-30.

Iversen JR, Repp BH, Patel AD (2009): Top-down control of rhythm perception modulates early auditory responses. Annals of the New York Academy of Sciences. 1169(1):58-73.

Jenkinson N, Brown P (2011): New insights into the relationship between dopamine, beta oscillations and motor function. Trends in neurosciences. 34(12):611-8.

Jerbi K, Lachaux JP, Karim N, Pantazis D, Leahy RM, Garnero L, Baillet S. Coherent neural representation of hand speed in humans revealed by MEG imaging (2007): Proceedings of the National

Academy of Sciences. 104(18):7676-81.

Kalcher J, Pfurtscheller G (1995): Discrimination between phase-locked and non-phase-locked event-related EEG activity. Electroencephalography and clinical neurophysiology. 94(5):381-4.

Kelly CW, Sober SJ (2014): Frontiers in integrative neuroscience. 8.

Koelewijn T, van Schie HT, Bekkering H, Oostenveld R, Jensen O (2008): Motor-cortical beta oscillations are modulated by correctness of observed action. Neuroimage. 40(2):767-75.

Kort NS, Nagarajan SS, Houde JF (2014): A bilateral cortical network responds to pitch perturbations in speech feedback. Neuroimage. 86:525-35.

Lashley KS (1951): The problem of serial order in behavior.

Lehéricy S, Benali H, Van de Moortele PF, Pélégrini-Issac M, Waechter T, Ugurbil K, Doyon J (2005): Distinct basal ganglia territories are engaged in early and advanced motor sequence learning. Proceedings of the National Academy of Sciences of the United States of America. 102(35):12566-71.

Leventhal DK, Gage GJ, Schmidt R, Pettibone JR, Case AC, Berke JD (2012): Basal ganglia beta oscillations accompany cue utilization. Neuron.73(3):523-36.

Lopes da Silva FH, Pfurtscheller G (1999): Basic concepts on EEG synchronization and desynchronization. Handbook of Electroencephalogr and Clinical Neurophysiology. 6: 3–11.

Luft CD (2014): Learning from feedback: The neural mechanisms of feedback processing facilitating better performance. Behavioural brain research. 261:356-68.

Maidhof C, Vavatzanidis N, Prinz W, Rieger M, Koelsch S (2010): Processing expectancy violations during music performance and perception: an ERP study. Journal of Cognitive Neuroscience. 22(10):2401-13.

Maris E, Oostenveld R (2007): Nonparametric statistical testing of EEG-and MEG-data. Journal of neuroscience methods. 164(1):177-90.

Martin T, Houck JM, Bish JP, Kičić D, Woodruff CC, Moses SN, Lee DC, Tesche CD (2006): MEG

reveals different contributions of somatomotor cortex and cerebellum to simple reaction time after temporally structured cues. Human brain mapping. 27(7):552-61.

Molinari M, Leggio MG, Solida A, Ciorra R, Misciagna S, Silveri MC, Petrosini L (1997): Cerebellum and procedural learning: evidence from focal cerebellar lesions. Brain. 120(10):1753-62.

Muthukumaraswamy S (2013): High-frequency brain activity and muscle artifacts in MEG/EEG: a review and recommendations. Frontiers in human neuroscience. 7: 138.

Natke U, Donath TM, Kalveram KT (2003): Control of voice fundamental frequency in speaking versus singing. The Journal of the Acoustical Society of America.113(3):1587-93.

Neumann WJ, Jha A, Bock A, Huebl J, Horn A, Schneider GH, Sander TH, Litvak V, Kühn AA (2015): Cortico-pallidal oscillatory connectivity in patients with dystonia. Brain. 138(7):1894-906.

Nieder A (2012): Supramodal numerosity selectivity of neurons in primate prefrontal and posterior parietal cortices. Proceedings of the National Academy of Sciences. 109(29):11860-5.

Nierula B, Hohlefeld FU, Curio G, Nikulin VV (2013): No somatotopy of sensorimotor alpha-oscillation responses to differential finger stimulation. Neuroimage. 76:294-303.

Nieuwenhuis S, Holroyd CB, Mol N, Coles MG (2004): Reinforcement-related brain potentials from medial frontal cortex: origins and functional significance. Neuroscience & Biobehavioral Reviews. 28(4):441-8.

Ninokura Y, Mushiake H, Tanji J (2004): Integration of temporal order and object information in the monkey lateral prefrontal cortex. Journal of neurophysiology. 91(1):555-60.

Oostenveld R, Fries P, Maris E, Schoffelen JM (2010): FieldTrip: open source software for advanced analysis of MEG, EEG, and invasive electrophysiological data. Computational intelligence and neuroscience (2011):

Oswal A, Litvak V, Sauleau P, Brown P (2012): Beta reactivity, prospective facilitation of executive processing, and its dependence on dopaminergic therapy in Parkinson's disease. The Journal of

Neuroscience. 32(29):9909-16.

Parkkonen L, Fujiki N, Mäkelä JP (2009): Sources of auditory brainstem responses revisited: contribution by magnetoencephalography. Human brain mapping. 30(6):1772-82.

Parvizi J, Van Hoesen GW, Buckwalter J, Damasio A (2006): Neural connections of the posteromedial cortex in the macaque. Proceedings of the National Academy of Sciences. 103(5):1563-8.

Patel AD (2011): Why would musical training benefit the neural encoding of speech? The OPERA hypothesis. The relationship between music and language. 195.

Petrides M (1991): Functional specialization within the dorsolateral frontal cortex for serial order memory. Proceedings of the Royal Society of London B: Biological Sciences. 246(1317):299-306.

Petrides M, Pandya DN (1999): Dorsolateral prefrontal cortex: comparative cytoarchitectonic analysis in the human and the macaque brain and corticocortical connection patterns. European Journal of Neuroscience. 11(3):1011-36.

Pfordresher PQ, Mantell JT, Brown S, Zivadinov R, Cox JL (2014): Brain responses to altered auditory feedback during musical keyboard production: an fMRI study. Brain research. 1556:28-37.

Pfordresher PQ, Palmer C (2006): Effects of hearing the past, present, or future during music performance. Perception & Psychophysics. 68(3):362-76.

Pollok B, Südmeyer M, Gross J, Schnitzler A (2005): The oscillatory network of simple repetitive bimanual movements. Cognitive brain research. 25(1):300-11.

Procyk E, Joseph JP (2001): Characterization of serial order encoding in the monkey anterior cingulate sulcus. European Journal of Neuroscience. 14(6):1041-6.

Restuccia D, Della Marca G, Valeriani M, Leggio MG, Molinari M (2007): Cerebellar damage impairs detection of somatosensory input changes. A somatosensory mismatch-negativity study. Brain. 130(1):276-87.

Ridderinkhof KR, Ullsperger M, Crone EA, Nieuwenhuis S (2004):The role of the medial frontal

cortex in cognitive control. Science. 306:443– 447.

Rinne T, Alho K, Ilmoniemi RJ, Virtanen J, Näätänen R (2000): Separate time behaviors of the temporal and frontal mismatch negativity sources. Neuroimage. 12(1):14-9.

Rushworth MF, Behrens TE (2008): Choice, uncertainty and value in prefrontal and cingulate cortex. Nature neuroscience. 11(4):389-97.

Saunders B, Jentzsch I (2012): False external feedback modulates posterror slowing and the f-P300: implications for theories of posterror adjustment. Psychonomic bulletin & review. 19(6):1210-6.

Sober SJ, Brainard MS (2012): Vocal learning is constrained by the statistics of sensorimotor experience. Proceedings of the National Academy of Sciences. 109(51):21099-103.

Swann N, Tandon N, Canolty R, Ellmore TM, McEvoy LK, Dreyer S, DiSano M, Aron AR (2009): Intracranial EEG reveals a time-and frequency-specific role for the right inferior frontal gyrus and primary motor cortex in stopping initiated responses. The Journal of neuroscience. 29(40):12675-85.

Tan H, Jenkinson N, Brown P (2014): Dynamic neural correlates of motor error monitoring and adaptation during trial-to-trial learning. The Journal of Neuroscience. 34(16):5678-88.

Tanji J, Shima K (1994): Role for supplementary motor area cells in planning several movements ahead. Nature 371:413–416.

Taulu S, Kajola M, Simola J (2004): Suppression of interference and artifacts by the signal space separation method. Brain topography. 16(4):269-75.

Taulu S, Simola J (2006): Spatiotemporal signal space separation method for rejecting nearby interference in MEG measurements. Physics in medicine and biology. 51(7):1759.

Taulu S, Kajola M (2005): Presentation of electromagnetic multichannel data: the signal space separation method. Journal of Applied Physics. 97(12):124905.

Tesche CD, Karhu J (1997): Somatosensory evoked magnetic fields arising from sources in the human cerebellum. Brain Res. 744: 23–31.

Tesche CD, Karhu JJ (2000b): Anticipatory cerebellar responses during somatosensory omission in man. Hum Brain Mapp. 9: 119–42.

Tierney A, Dick F, Deutsch D, Sereno M (2013): Speech versus song: multiple pitch-sensitive areas revealed by a naturally occurring musical illusion. Cerebral Cortex. 23(2):249-54.

Torrecillos F, Alayrangues J, Kilavik BE, Malfait N (2015): Distinct Modulations in Sensorimotor Postmovement and Foreperiod β-Band Activities Related to Error Salience Processing and Sensorimotor Adaptation. The Journal of Neuroscience. 35(37):12753-65.

Tourville JA, Reilly KJ, Guenther FH (2008): Neural mechanisms underlying auditory feedback control of speech. Neuroimage. 39(3):1429-43.

Tzourio-Mazoyer N, Landeau B, Papathanassiou D, Crivello F, Etard O, Delcroix N, Mazoyer B, Joliot M (2002): Automated anatomical labeling of activations in SPM using a macroscopic anatomical parcellation of the MNI MRI single-subject brain. Neuroimage. 15(1):273-89.

Vogt BA, Pandya DN (1987): Cingulate cortex of the rhesus monkey: II. Cortical afferents. Journal of Comparative Neurology. 262(2):271-89.

Wiestler T, Diedrichsen J (2013): Skill learning strengthens cortical representations of motor sequences. eLife 2:e00801.

Wolpert DM, Ghahramani Z, Flanagan JR (2001): Perspectives and problems in motor learning. Trends in cognitive sciences. 5(11):487-94.

Zarate JM (2013): The neural control of singing. Frontiers in human neuroscience. 7.

Zarate JM, Zatorre RJ (2008): Experience-dependent neural substrates involved in vocal pitch regulation during singing. Neuroimage. 40(4):1871-87.

Zatorre RJ, Baum SR (2012): Musical melody and speech intonation: Singing a different tune. PLoS Biol. 10(7):e1001372.

Zhang Y, Chen Y, Bressler SL, Ding M (2008): Response preparation and inhibition: the role of the

cortical sensorimotor beta rhythm. Neuroscience. 156(1):238-46.

Figure Legends

Figure 1. Experimental Paradigm

A. Scheme of one trial of the experimental paradigm. Time course of the presentation of the initial visual cue with the image of the piano and the block-specific sequence content, followed by the auditory cues. The auditory cues reproduced the sequence elements for two renditions at a rate of one tone every 300 ms (200 bpm) *prior* to the go signal. Participants had to begin playing the sequence renditions after the last metronome cue at the presentation of the go cue (green ellipse). Within-trial performance was characterized by a concatenation of approximately 10 sequence renditions without large pauses. The end of the trial after 23 s of performance was signaled by a visual cue with a red ellipse. **B.** The pitch content (and corresponding MIDI note numbers) of our custom-made MEG-compatible keyboard is displayed at the bottom. During the experiment we used three kinds of auditory feedback. (i) Normal auditory feedback associated with the keystroke (NAF, denoted here by the black quaver) was present in the control trials (1, 6, 11). (ii) Alterations of auditory feedback sounding as a serial order error (alterations of serial order or ASO, denoted by the blue quaver) were introduced in trials 2, 4, 8, 10, 12, 14. (iii) Alterations of auditory feedback with a pitch content unrelated to the sequence (unrelated auditory feedback alterations or UAF, with pitch values $A^{\#}$ or $D^{\#}$ and corresponding MIDI note numbers 59 and 64; denoted by the red quaver) were introduced in trials 3, 5, 7, 9, 13, 15.

Figure 2. Behavioral Data

A. Rate of self-produced pitch errors (and SEM bars) in trials with normal feedback or NAF (#1, 6, 11), alterations of serial order or ASO (#2, 4, 8, 10, 12, 14) and unrelated auditory feedback or UAF (#3, 5, 7, 9, 13, 15). The star indicates that the pitch error rate in ASO trials, but not in UAF trials, was significantly larger

than the rate in trials with NAF ($p < pth = 0.01$). **B.** The average inter-onset-interval (mIOI in ms; and SEM bars) at keystrokes with NAF, ASO or UAF, and at keystrokes following alterations of auditory feedback of each kind at +1 (postASO, postUAF) or +2 (post2ASO, post2UAF) positions is displayed. The star denotes the significantly larger mean IOI obtained in keystrokes following UAF or ASO feedback ($p < pth = 0.018$).

Figure 3. Effects of alterations of auditory feedback (AAF) on oscillatory power in the sensor-space. Magnetometers.

Top row shows scalp topographies for relative power changes in the theta (4-7Hz , left & center) and beta band (13-30Hz, right), corresponding to the significant clusters obtained within 150 to 400 ms (0 ms is keystroke and auditory feedback onset; cluster permutation test, $p < 0.025$, two-sided test) for the different between-condition comparisons. The black stars denote the sensors belonging to the significant clusters. Power values are provided as relative power change (subtraction and division by the reference baseline average: dimensionless units). The left map presents the comparison between trials with serial order alterations (ASO) and normal feedback (NAF), revealing a significant positive cluster in the theta frequency region. The center map reveals a significant positive cluster in the theta band with a *right frontoparietal* scalp distribution, corresponding to the comparison between trials with unrelated auditory feedback alterations (UAF) and normal feedback (NAF). The right map displays a comparison between ASO and UAF trials, demonstrating a significant positive cluster in the beta band, which had a *left frontal* scalp distribution. Lower row shows some time courses of the cluster-based power averaged within the corresponding significant frequency band and the sensors pertaining to the significant positive clusters shown above.

Figure 4. CSP and source localization of theta oscillatory activity in magnetometers for the ASO-NAF difference.

A-C. Theta-band CSP patterns (in a.u.) obtained for the three largest eigenvalues from two representative

subjects (upper row: subject #5, lower row: subject #11). These CSP patterns corresponded to an enhanced theta-band oscillatory activity in the ASO as compared to the normal feedback condition and were generated by a monopolar source in the cingulum (**A**), a dipolar source in the cerebellum (**B**) or in the temporal gyrus **(C)**. **D-F.** Location of the standard MNI coordinates (median and median absolute dispersion across subjects) of the anatomical locations of the dipoles generating the CSP patterns obtained for each between-condition difference in the sensor space (represented in the upper panels). Sagittal and coronal projections.

Figure 5. CSP and source localization of theta oscillatory activity in magnetometers for the UAF-NAF difference.

Theta-band CSP patterns (a.u.) obtained for **two** of the three largest eigenvalues from the same representative subjects as in **Figure 4.** These CSP patterns corresponded to an enhanced theta-band oscillatory activity in the UAF as compared to the normal feedback condition and were generated by a monopolar source in the cerebellum (**A**), or a dipolar source in the temporal gyrus **(B)**. **(C-D)** Location of the standard MNI coordinates (median and median absolute dispersion across subjects) of the anatomical locations of the dipoles generating the CSP patterns obtained for each between-condition difference in the sensor space (represented in the upper panels). Sagittal and coronal projections.

Figure 6. CSP and source localization of beta oscillatory activity in magnetometers for the ASO-UAF difference. (A-C) CSP patterns (in a.u.) from two representative subjects (upper row: subject #3; lower row: subject #16) in association with two of the three largest eigenvalues, and corresponding to the maximization of variance of beta oscillatory activity in the modified feedback condition ASO as compared to UAF. The representative beta-band CSP patterns were generated by sources in the cingulate gyrus **(A)** and the cerebellum **(B)**. **(C-D)** The anatomical locations of the dipoles generating the beta-band CSP patterns are provided as median and median absolute dispersion across subjects in standard MNI coordinates. Sagittal

and coronal projections.

Figure 7. Correlation of behavioral data with oscillatory activity at the source level. Correlation across subjects (Spearman ρ) of the magnitude of the dipole moment (nAm) in the cingulate cortex leading to the ASO-UAF difference in beta-band oscillatory activity (x-axis) and the difference in pitch error rates (y-axis). Larger error rates in ASO relative to UAF epochs were associated across subjects with higher cingulate beta-band activity.

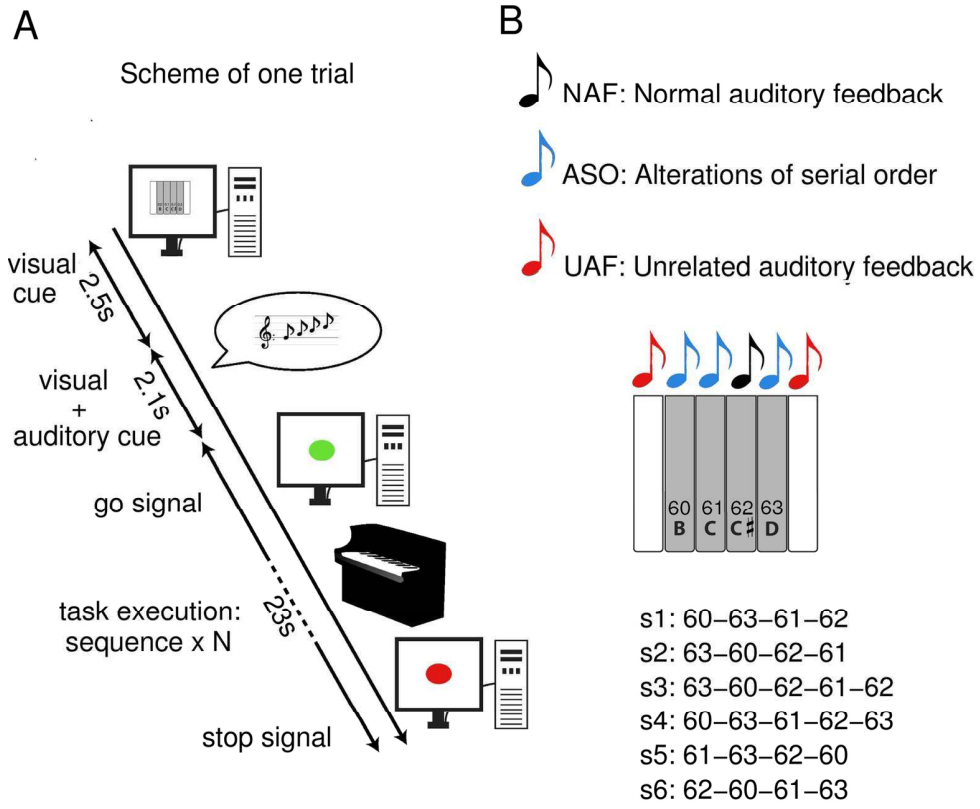

Figure 1. Experimental Paradigm. A. Scheme of one trial of the experimental paradigm. Time course of the presentation of the initial visual cue with the image of the piano and the block-specific sequence content, followed by the auditory cues. The auditory cues reproduced the sequence elements for two renditions at a rate of one tone every 300 ms (200 bpm) prior to the go signal. Participants had to begin playing the sequence renditions after the last metronome cue at the presentation of the go cue (green ellipse). Within-trial performance was characterized by a concatenation of approximately 10 sequence renditions without large pauses. The end of the trial after 23 s of performance was signaled by a visual cue with a red ellipse. B. The pitch content (and corresponding MIDI note numbers) of our custom-made MEG-compatible keyboard is displayed at the bottom. During the experiment we used three kinds of auditory feedback. (i) Normal auditory feedback associated with the keystroke (NAF, denoted here by the black quaver) was present in the control trials (1, 6, 11). (ii) Alterations of auditory feedback sounding as a serial order error (alterations of serial order or ASO, denoted by the blue quaver) were introduced in trials 2, 4, 8, 10, 12, 14. (iii) Alterations of auditory feedback with a pitch content unrelated to the sequence (unrelated auditory feedback alterations or UAF, with pitch values A# or D# and corresponding MIDI note numbers 59 and 64; denoted by the red quaver) were introduced in trials 3, 5, 7, 9, 13, 15.

150x125mm (300 x 300 DPI)

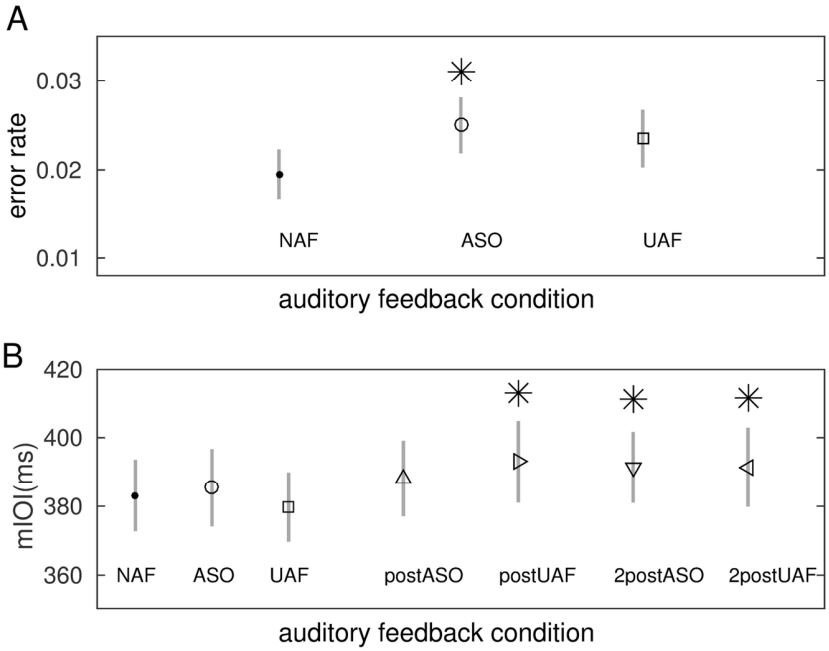

Figure 2. Behavioral Data
A. Rate of self-produced pitch errors (and SEM bars) in trials with normal feedback or NAF (#1, 6, 11), alterations of serial order or ASO (#2, 4, 8, 10, 12, 14) and unrelated auditory feedback or UAF (#3, 5, 7, 9, 13, 15). The star indicates that the pitch error rate in ASO trials, but not in UAF trials, was significantly larger than the rate in trials with NAF ($p < pth = 0.01$). B. The average inter-onset-interval (mIOI in ms; and SEM bars) at keystrokes with NAF, ASO or UAF, and at keystrokes following alterations of auditory feedback of each kind at +1 (postASO, postUAF) or +2 (post2ASO, post2UAF) positions is displayed. The star denotes the significantly larger mean IOI obtained in keystrokes following UAF or ASO feedback ($p < pth = 0.018$).

150x109mm (300 x 300 DPI)

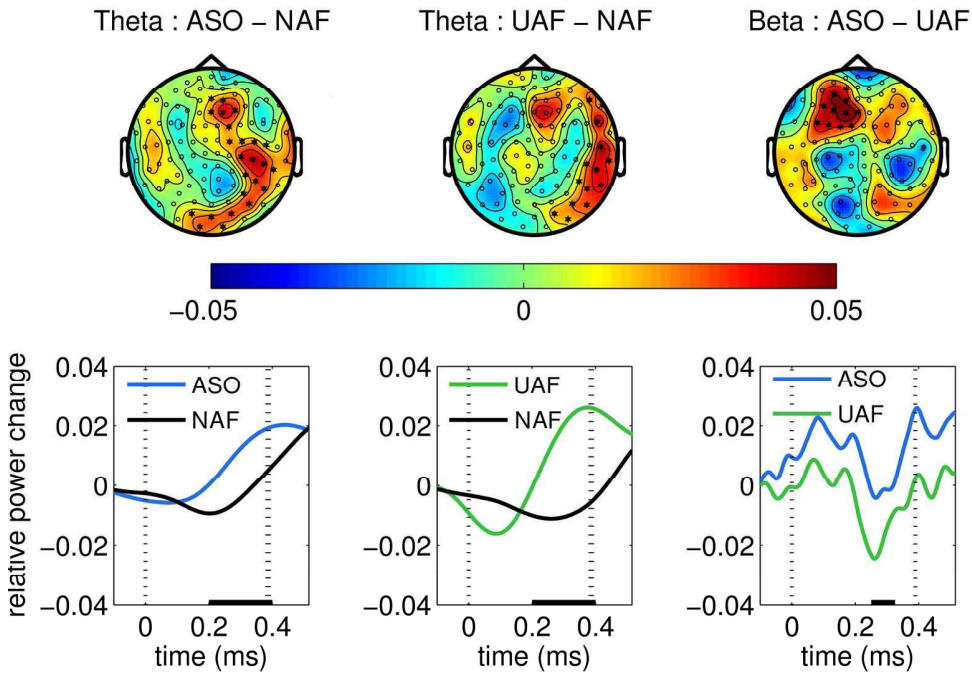

Figure 3. Effects of alterations of auditory feedback (AAF) on oscillatory power in the sensor-space. Magnetometers. Top row shows scalp topographies for relative power changes in the theta (4-7Hz , left & center) and beta band (13-30Hz, right), corresponding to the significant clusters obtained within 150 to 400 ms (0 ms is keystroke and auditory feedback onset; cluster permutation test, $p < 0.025$, two-sided test) for the different between-condition comparisons. The black stars denote the sensors belonging to the significant clusters. Power values are provided as relative power change (subtraction and division by the reference baseline average: dimensionless units). The left map presents the comparison between trials with serial order alterations (ASO) and normal feedback (NAF), revealing a significant positive cluster in the theta frequency region. The center map reveals a significant positive cluster in the theta band with a right frontoparietal scalp distribution, corresponding to the comparison between trials with unrelated auditory feedback alterations (UAF) and normal feedback (NAF). The right map displays a comparison between ASO and UAF trials, demonstrating a significant positive cluster in the beta band, which had a left frontal scalp distribution. Lower row shows some time courses of the cluster-based power averaged within the corresponding significant frequency band and the sensors pertaining to the significant positive clusters shown above.

176x123mm (300 x 300 DPI)

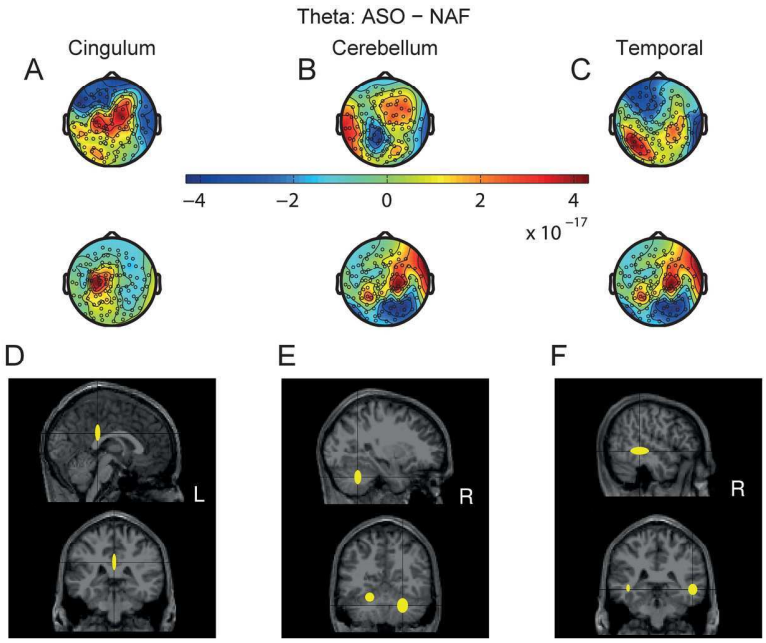

Caption : Figure 4. CSP and source localization of theta oscillatory activity in magnetometers for the ASO-NAF difference. A-C. Theta-band CSP patterns (in a.u.) obtained for the three largest eigenvalues from two representative subjects (upper row: subject #5, lower row: subject #11). These CSP patterns corresponded to an enhanced theta-band oscillatory activity in the ASO as compared to the normal feedback condition and were generated by a monopolar source in the cingulum (A), a dipolar source in the cerebellum (B) or in the temporal gyrus (C). D-F. Location of the standard MNI coordinates (median and median absolute dispersion across subjects) of the anatomical locations of the dipoles generating the CSP patterns obtained for each between-condition difference in the sensor space (represented in the upper panels). Sagittal and coronal projections.

173x130mm (300 x 300 DPI)

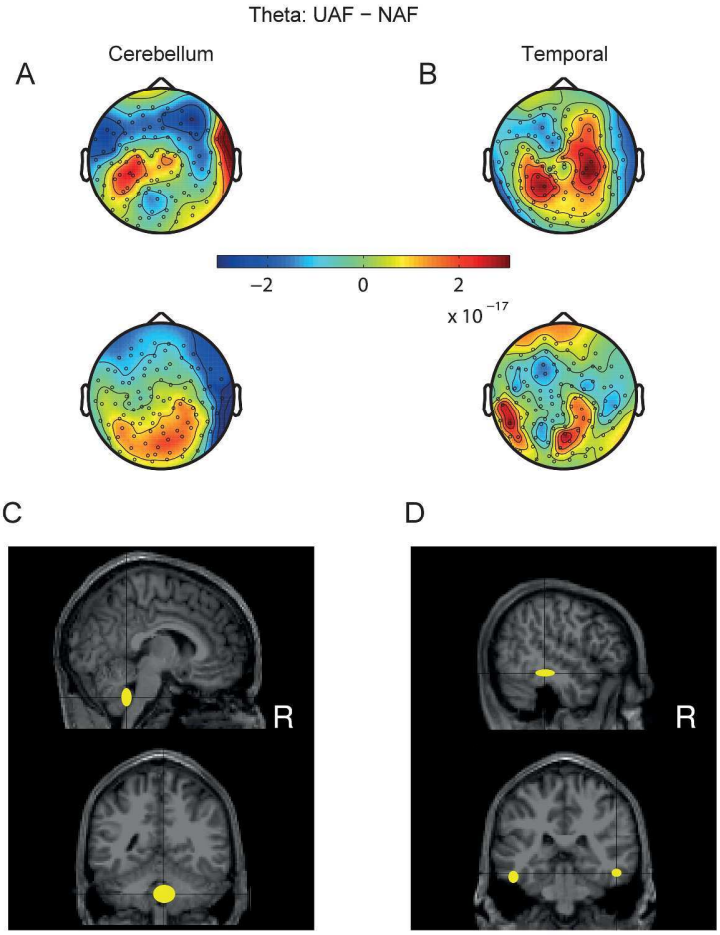

Figure 5. CSP and source localization of theta oscillatory activity in magnetometers for the UAF-NAF difference. Theta-band CSP patterns (a.u.) obtained for two of the three largest eigenvalues from the same representative subjects as in Figure 4. These CSP patterns corresponded to an enhanced theta-band oscillatory activity in the UAF as compared to the normal feedback condition and were generated by a monopolar source in the cerebellum (A), or a dipolar source in the temporal gyrus (B). (C-D) Location of the standard MNI coordinates (median and median absolute dispersion across subjects) of the anatomical locations of the dipoles generating the CSP patterns obtained for each between-condition difference in the sensor space (represented in the upper panels). Sagittal and coronal projections.

279x361mm (300 x 300 DPI)

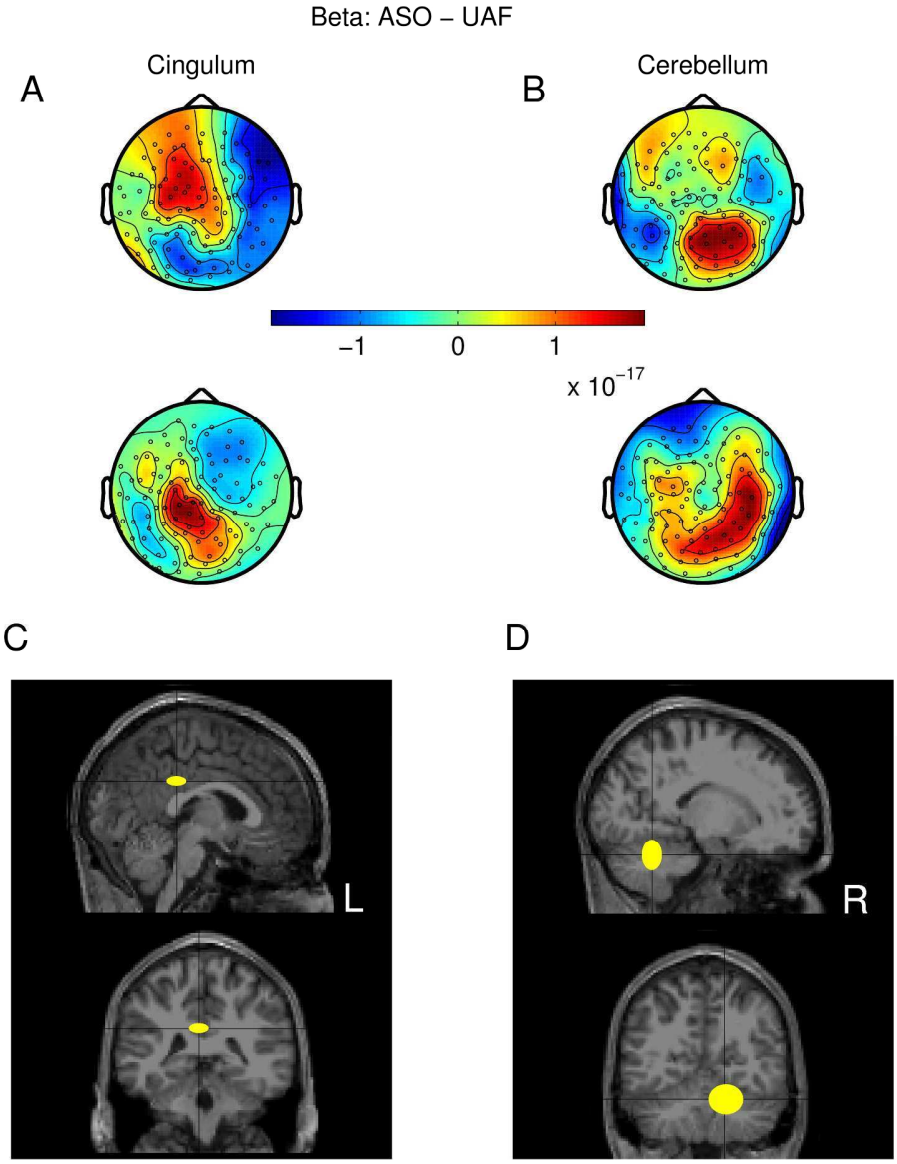

Figure 6. CSP and source localization of beta oscillatory activity in magnetometers for the ASO-UAF difference. (A-C) CSP patterns (in a.u.) from two representative subjects (upper row: subject #3; lower row: subject #16) in association with two of the three largest eigenvalues, and corresponding to the maximization of variance of beta oscillatory activity in the modified feedback condition ASO as compared to UAF. The representative beta-band CSP patterns were generated by sources in the cingulate gyrus (A) and the cerebellum (B). (C-D) The anatomical locations of the dipoles generating the beta-band CSP patterns are provided as median and median absolute dispersion across subjects in standard MNI coordinates. Sagittal and coronal projections.

224x290mm (300 x 300 DPI)

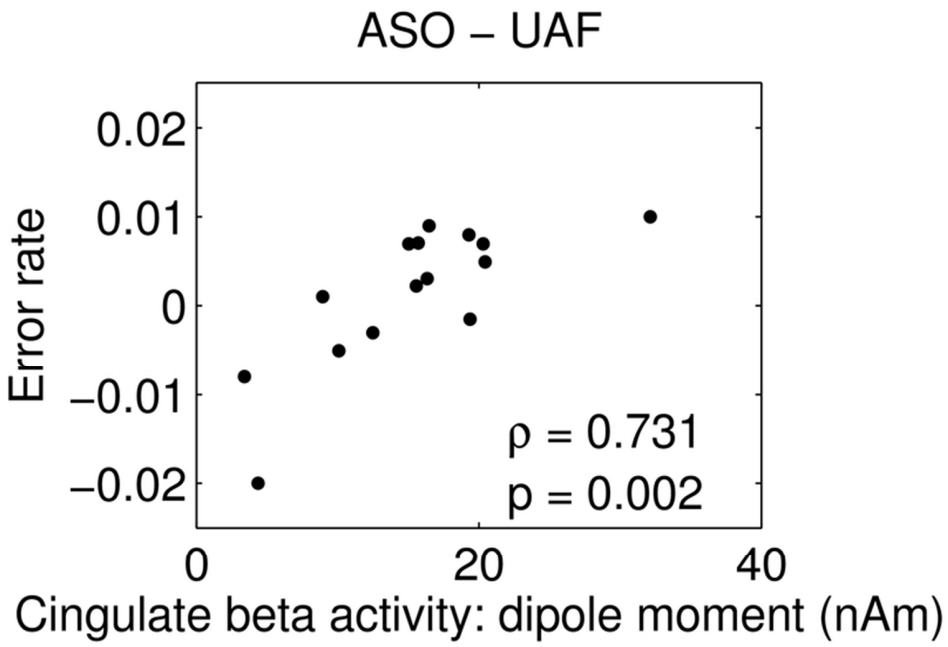

Figure 7. Correlation of behavioral data with oscillatory activity at the source level. Correlation across subjects (Spearman ρ) of the magnitude of the dipole moment (nAm) in the cingulate cortex leading to the ASO-UAF difference in beta-band oscillatory activity (x-axis) and the difference in pitch error rates (y-axis). Larger error rates in ASO relative to UAF epochs were associated across subjects with higher cingulate beta-band activity.

70x48mm (300 x 300 DPI)

For Review

Supplementary Material: Cingulate and Cerebellar Beta Oscillations are Engaged in the Acquisition of Auditory-Motor Sequences

Table of Contents for Supplementary Material

1. Supplementary Methods

Statistical Analysis

In the statistical analysis of behavioural results using non-parametric paired permutation tests, we also report a non-parametric effect size estimator, PS_{dep}, following Grissom and Kim (2012). PS_{dep} is the probability that in a randomly sampled pair of *dependent* values (one matched pair: two values from the same participant under different conditions) the value from Condition B (which for instance has larger values) will be greater than the value from Condition A. The maximum value is $PS_{dep} = 1$. Since a paired permutation test permutes the sign of pairs of samples (sign test), we can proceed as follows: for two samples of length N, we first compute the difference between each of the N pairs of values from both samples, then we count the number of positive difference scores

N+. The probability of greater values in sample B relative to A is PS_{dep} = N+ /N. If there are ties (zero difference), we reduce the denominator N by the number of ties N0 (PS_{dep} = N+ /[N-N0]). A non-parametric estimation of effect size like PS_{dep} is more adequate when using non-parametric tests than reporting parametric effect size estimates such as Cohen's d, particularly because parametric effect size estimates are affected by deviations from normality and heterogeneity of variances.

Source reconstruction

The CSP algorithm (Blankertz et al. 2008) is a method used to analyze multi-channel data based on recordings from two conditions. CSP leads to the generalized eigenvalue decomposition of the original signal $x(t) \in \mathbb{R}^C$ into $x_{CSP}(t) \in \mathbb{R}^C$. The decomposition is parameterized by a matrix $W \in \mathbb{R}^{CxC}$ (C being the number of channels) as follows:

$$x_{CSP}(t) = W^T x(t) \quad (1)$$

Following e.g. Blankertz et al. (2008), we call each column vector $w_j(t) \in \mathbb{R}^C$ (j = 1,...,C) of W a *spatial filter* and each column vector $a_j(t) \in \mathbb{R}^C$ of the inverse matrix $A = W^{-1}$ a *spatial pattern.* The way in which matrix W is obtained follows an optimization criterion, such that CSP filters maximize the variance of the spatially filtered signal for one condition while minimizing it for the other condition.

The CSP components can be obtained by projecting the original sensor-space signals X using spatial filters in W:

$$Z = WX$$

The projected data in Z contain components (sources) and are sorted by the size of their

eigenvalue (from high to low).

Thus, the spatial patterns a_j can be viewed as a correlation map between original sensor signal x_i and the spatially filtered signal z_j (sources).

As in Nierula et al. (2013), we performed source reconstruction with current equivalent dipole modeling using the CSP patterns a_j associated with the three largest eigenvalues in each subject.

Statistics of inverse calculations: We tested the null hypothesis that across subjects the fitted dipoles could be located across all grid positions (in MNI space) with the same probability. To this aim we assumed that the probability of fitting a dipole to any point *j* within the individual warped grid was uniformly distributed ($p_j = 1/N_{grid}$, with $N_{grid} = 37163$ the total number of grid points inside the subject-specific space). Next, we assessed the probability of grid points, p_{loc}, falling within each anatomical location from the AAL atlas. Our locations of interest were the cingulate gyrus, the temporal gyrus, the cerebellum, the SMA and the functional area of the dorsolateral prefrontal cortex (DLPFC): (contributing to the anatomical area of the middle frontal gyrus: labels Frontal_Sup and Frontal_Mid n the AAL atlas; Brodmann areas 9 and 46). For each of those locations, we treated the results as a *binomial experimen*t consisting of a fixed number n of statistically independent Bernoulli trials (n = 20 subjects), each with a probability of success p_{loc}, and we counted the number of successes *k* (meaning *k* subjects exhibited that location after dipole fitting).

In a binomial experiment, the probability of *k* successes out of a sample of *n* independent variables (subjects) is determined by the binomial distribution

$$P(\mathrm{k,n}) = \binom{n}{p_{\mathrm{loc}}} p_{\mathrm{loc}}^{k} q_{\mathrm{loc}}^{(n-k)} \qquad (2)$$

With q_{loc} being the probability of failure in the experiment $q_{\mathrm{loc}} = 1 - p_{\mathrm{loc}}$. Now, considering that for

each subject we fitted a dipole to each of the 3 CSP and assuming that these CSP are independent among them (implying that each CSP leads to a different location), the probability of success of one location being found for at least one of the 3 CSP is $p_3 = 1 - (q_{\mathrm{loc}})^3$ and $q_3 = 1 - p_3$. Accordingly, the probability that at least *k* subjects out of *n* have a source in the same specific location *loc* is

$$P(\mathrm{k,n}) = \sum_{k'=k}^{n} \binom{n}{p_3} p_3^{k'^{(n-k')}} \tag{3}$$

The final p-value was corrected for multiple comparisons arising from the five locations of interest by using the Bonferroni correction: $\alpha / 5 = 0.01$, with $\alpha = 0.05$. Accordingly, the null hypothesis was rejected for any of the locations being tested whenever there was at least the minimum number of subjects *k* showing that same specific location, with a probability P(k,n) below the corrected significance threshold 0.01.

2. Supplementary Results

Questionnaire data

After completing all performance blocks, participants filled out questionnaires asking them about their subjective error number estimates and their awareness of the different kinds of alterations of auditory feedback (AAF). The questions included in the questionnaire were:

Please, answer whether the following statements are CORRECT or WRONG.
[ ] 1a. I produced fewer than ten errors per block by pressing a wrong key.
[ ] 1b. I produced more than ten errors but fewer than twenty errors per block by pressing a wrong

key.

[ ] 1c. I produced more than twenty errors per block by pressing a wrong key.

[ ] 2. I realised that I made errors because the note was different than expected.

[ ] 3. I realised that I made errors because the movement felt different than expected.

[ ] 4. I memorized the sequence of keystrokes ignoring the tones.

[ ] 5. I realised that the auditory feedback was occasionally modified.

[ ] 6. I think that I always managed to realise when auditory feedback was externally modified.

[ ] 7. I realised that some altered tones produced by the computer corresponded to elements from the sequence I was playing.

[ ] 8. I realised that some altered tones produced by the computer were completely unrelated to the sequence I was playing.

Based on the answers provided in questions 1a-1c, we scored their estimated error number (per sequence type) as:

If 1a TRUE → 5 errors per sequence type

If 1b TRUE → 15 errors per sequence type

If 1c TRUE → 25 errors per sequence type

Participant #6 marked two options as true: 1b and 1c. Accordingly, we assigned an error number estimate of 20 to this participant.

The subjective estimate of self-produced error per sequence type was on average 19 (1), whereas the number of self-produced errors was 15 (2), and the difference was significant ($p = 0.016$). Thus, participants overestimated the number of pitch errors due to the presence of AAF, an outcome that

has been reported in a previous behavioral study (Pfordrescher and Beasley, 2014).

The following table indicates the number of participants (N = 20) marking the questionnaire items 2-8 as true statements:

Questionnaire item	Number of participants selecting TRUE (Ntotal = 20)
2	9
3	18
4	14
5	18
6	12
7	13
8	16

Based on participant's responses, it seems that they might have preferred movement-based over auditory-based error detection (item 3 vs 2), as well as have aimed at learning the sequences without paying may much attention to the auditory information. Significantly, however, the large majority of the participants retrospectively reported to have noticed the different kinds of AAF manipulations and have distinguished AAF from self-produced errors.

Improvements in performance during the familiarization session

During the familiarisation stage, participants exhibited significant improvements in performance timing across training trials (1 to 3): reduced average tempo, 420 [10] ms and 385 [10] ms, p = = 10^{-3}, PS_{dep} = 0.95; reduced temporal variability 0.28 [0.03] to 0.25 [0.03], p = 0.01, PS_{dep} = 0.75.

In addition, in the first trial of the performance block (normal feedback) there were additional improvements in performance relative to the last trial of the training block: reduced average tempo, 384 [9] ms and 378 [9] ms, p = 0.03, PS_{dep} = 0.70; reduced temporal variability, 0.25 [0.03] to 0.23

[0.02], p = 0.04, PS_{dep} = 0.65.

Thus, there were initial improvements in performance during the familiarisation phase, and further improvements in the first normal trial of the performance session. However, the introduction of AAF during the subsequent trials of this session disturbed learning. This converges with previous evidence supporting that a distractor task can suppress the performance changes associated with learning (Seidler et al., 2002).

Pitch errors induced by AAF

We assessed the properties of the self-produced pitch errors which may have been induced by AAF events (here termed 'AAF-induced-errors'). To this aim, we selected pitch errors that followed an AAF event and preceded the next one, with the constraint of a maximum distance of 10 keystrokes from previous AAF. Note that the average rate of AAF was one in every 8.37(0.05) keystrokes (same for ASO and UAF trials). Our stimulus material were sequences of 4 or 5 elements. Specifically, we looked into the three following properties:

1. Distance in number of keystrokes between the error and the previous AAF .

The AAF-induced-errors occurred between n+3 and n+5 keystrokes from the AAF (on average at 4.3 [0.1] subsequent keystrokes after ASO, and 4.5 [0.1] after UAF; n.s. difference between position in ASO and UAF trials, $p > 0.05$). This outcome indicated that AAF induced pitch errors at the same ordinal position of the current AAF (or one position before, i.e. anticipating a potential upcoming AAF) but in the next rendition of the sequence.

2. Distance in ordinal position between the event in which an AAF was introduced and the subsequent AAF-induced-error (Figure S4A).

The majority of the AAF-induced-errors, which occurred in the next rendition of the sequence, fell at the same (distance = 0) or at one earlier ordinal position (distance = -1) than the previous AAF event. In the latter case, the self-produced error anticipated with a lag 1 a potential repetition of an AAF event at the same ordinal position as it fell in the previous rendition. There was no significant difference between the proportion of distance values in ASO and UAF trials ($p > 0.05$ for all values).

3. Distance between the ordinal position that the AAF-induced-error activated (i.e. the wrong pitch activated an action of the sequence corresponding to an ordinal position 'ordpos_error') and the ordinal position in which the error occurred (i.e. the event which should have been played: 'ordpos_correct', See Figure S4B).

The largest proportion of the variable 'ordpos_error - ordpos_correct' was for a difference of 1, and the proportion was significantly larger in ASO relative to UAF trials (0.48 [0.03] and 0.40 [0.02], respectively, $p = 0.021$). This outcome indicated that the majority of the AAF-induced-errors were due to the anticipation of the pitch value of the next sequence element.

In sum, our detailed analysis of the properties of the AAF-induced-errors revealed the following main outcomes:

Participants compensated for the previous presence of (unpredicted) altered feedback by modifying the sequence contents in the next rendition. Specifically, the compensation mostly consisted of replacing the sequence element at the same or prior ordinal position in which the previous AAF fell ($m = n, n-1$; Figure S4A) with the anticipated subsequent sequence element ($m = n+1$ *or* n, respectively; Figure S4B). Moreover, this process occurred significantly more often following ASO events. Taken together these results indicate that participants altered the sequential organization of

the events planned for production to compensate for the previous AAF, and most often in the case of altered feedback simulating serial-order errors (ASO events). These outcomes are consistent with previous behavioral studies on sequential planning (e.g. Pfordrescher and Palmer, 2006), yet they are novel in demonstrating that – at least for short sequences – compensatory changes primarily occur in the next rendition of the sequence.

Additional results of the source localisation analysis

Here we report additional sources that were localised in a smaller number of participants following our CSP + dipole fitting procedure. These additional sources, however, were non-significant according to our statistical analysis at the group level. Below we present sources that were found in at least 5 participants.

For the ASO – NAF feedback comparison, additional sources of enhanced theta-band activity were located in a few subjects to the precentral gyrus (contralateral primary motor cortex, 8/20 subjects), dorsolateral and medial prefrontal cortex (7/20 and 6/20 subjects respectively), postcentral gyrus (contralateral somatosensory cortex, 6/20 subjects) and the thalamus (8/20 subjects).

For the UAF – NAF feedback comparison, additional sources of enhanced theta-band activity were located in a few subjects to the dorsolateral and medial prefrontal cortex (9/20 and 7/20 subjects respectively), the thalamus (7/20 subjects) and the cingulate cortex (6/20 subjects).

Finally, the effect of enhanced beta-band oscillatory activity obtained for the specific comparison between ASO and UAF trials was localized in a few subjects to the occipital lobe (9 / 20 subjects), the thalamus (8/20 subjects) and the temporal lobe (6/20 subjects).”

Finally, the effect of enhanced beta-band oscillatory activity obtained for the specific comparison

between ASO and UAF trials was localized in a few subjects to the occipital lobe (9 / 20 subjects, n.s.), the thalamus (8/20 subjects, n.s.) and the temporal lobe (6/20 subjects, n.s.)

3. **Supplementary Figures**

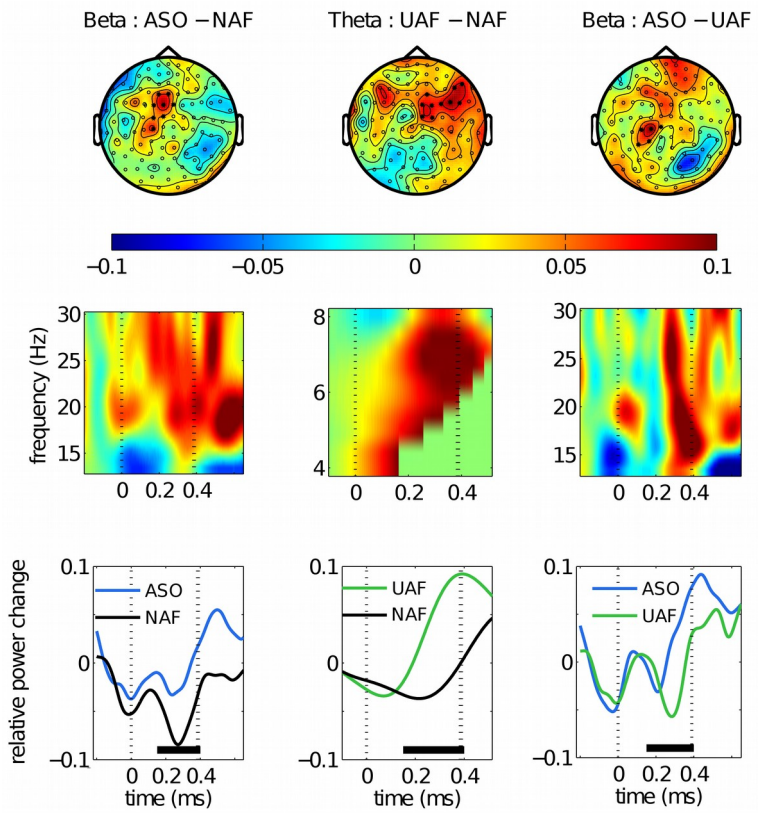

Figure S1. Effects of alterations of auditory feedback (AAF) on oscillatory power in the sensor-space. Planar gradiometers. Top row shows scalp topographies for relative power changes in the beta (left & right) and theta band (center), corresponding to the significant clusters obtained within 150 to 400 ms (0 ms is keystroke and auditory feedback onset; cluster permutation test, $p < 0.025$, two-sided test) for the different between-condition comparisons. Topographies are displayed in a combined planar gradiometer representation. The black stars denote the sensors belonging to the significant clusters. The left map presents the comparison between trials with serial order alterations (ASO) and normal feedback (NAF), revealing a significant positive cluster in the beta frequency region with a *midline frontocentral* scalp

distribution. The center map reveals a significant positive cluster in the theta band with a *right frontal* scalp distribution, corresponding to the comparison between trials with unrelated auditory feedback alterations (UAF) and NAF. The right map displays a comparison between ASO and UAF trials, demonstrating a significant positive cluster in the beta band, which had a *central* scalp distribution. Middle row shows grand-averages of the time-frequency power changes over the sensors pertaining to the significant positive clusters shown above. Lower row shows some time courses of the cluster-based power averaged within the corresponding significant frequency band as shown in the middle row.

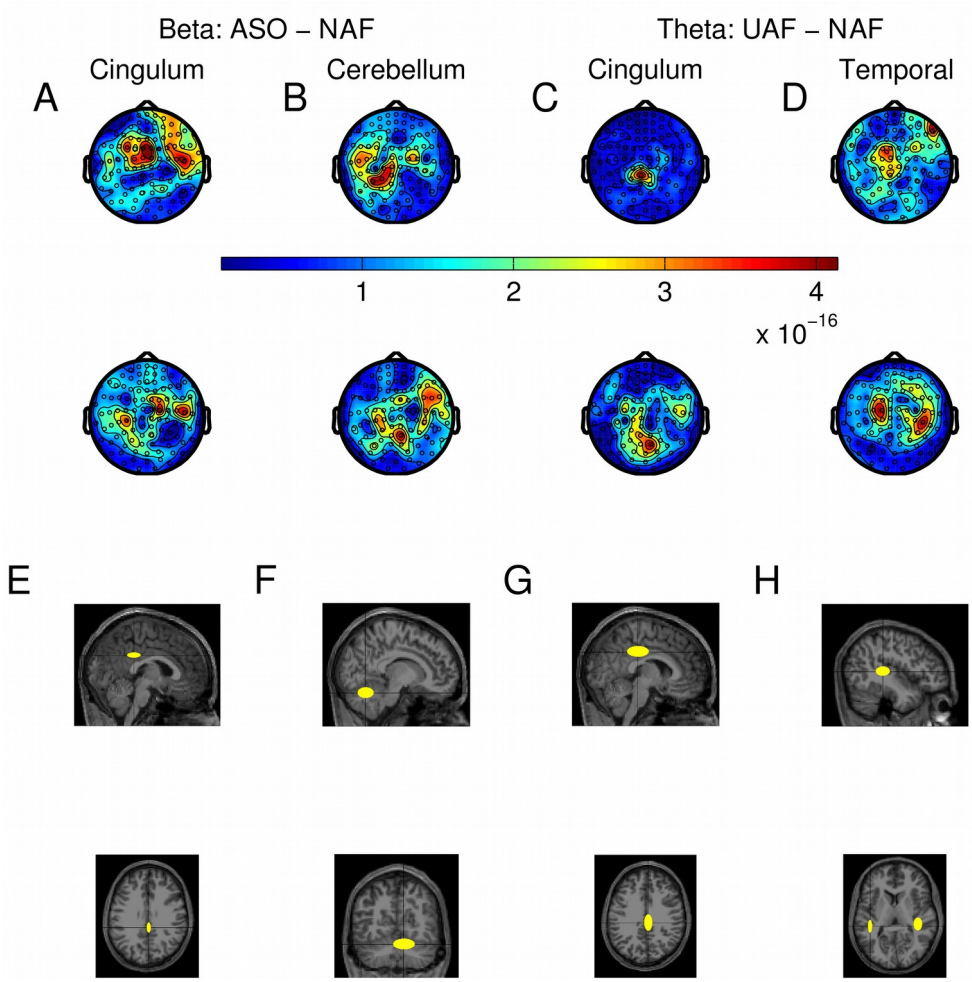

Figure S2. CSP and source localization of beta and theta oscillatory activity in planar gradiometers for the of ASO-NAF and UAF-NAF difference, respectively. A-B. Beta-band CSP patterns (in arbitrary

units, a.u.) obtained for one of the three largest eigenvalues from two representative subjects (upper row: subject #5, lower row: subject #10). These CSP patterns corresponded to an enhanced beta-band oscillatory activity in the ASO as compared to the normal feedback condition and were generated by a monopolar source in the cingulum (A) or cerebellum (B).The patterns are displayed in a combined planar gradiometer representation. C-D. Theta-band CSP patterns (in a.u.) obtained for one of the three largest eigenvalues from the same representative subjects as in (A-B). These CSP patterns corresponded to an enhanced theta-band oscillatory activity in the UAF as compared to the normal feedback condition and were generated by a monopolar source in the cingulum (A-B) or a dipolar source in the temporal gyrus (C-D). (E-H) Standard MNI coordinates (median and median absolute dispersion across subjects) of the anatomical locations of the dipoles generating the CSP patterns obtained for each between-condition difference in the sensor space (represented in the upper panels).

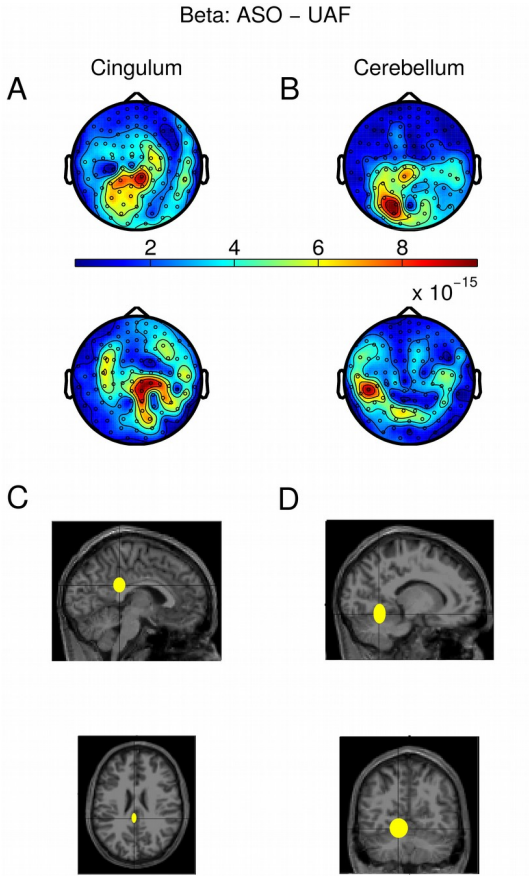

Figure S3. CSP and source localization of beta oscillatory activity in planar gradiometers for the of ASO-UAF difference. (A-B) CSP patterns (in a.u.) from two representative subjects (upper row: subject #12,; lower row: subject #17) in association with one of the three largest eigenvalues, and corresponding to the maximization of variance of beta oscillatory activity in the modified feedback condition ASO as compared to UAF. The representative beta-band CSP patterns were generated by sources in the cingulate gyrus (A) and the cerebellum (B). The patterns are displayed in a combined planar gradiometer representation. (C-D) The anatomical locations of the dipoles generating the beta-band CSP patterns are provided as median and median absolute dispersion across subjects in standard MNI coordinates.

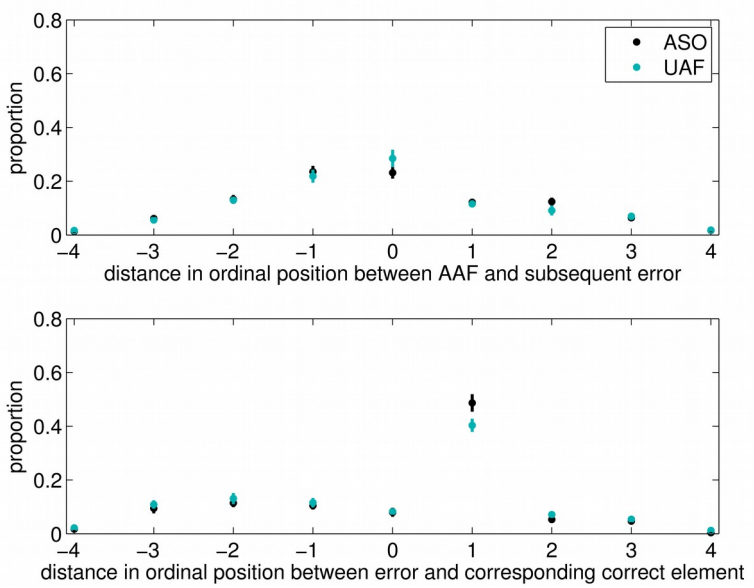

Figure S4. Proportion of values (and SEM bars) for the following variables: (A) Distance in ordinal position between the AAF event and the subsequent self-produced error (which ocurred in the next rendition of the sequence); (B) Distance between the ordinal position that the wrong pitch of the AAF-induced-error activated ('ordpos_error') and the ordinal position in which the error ocurred ('ordpos_correct'): ordpos_error – ordpos_correct.

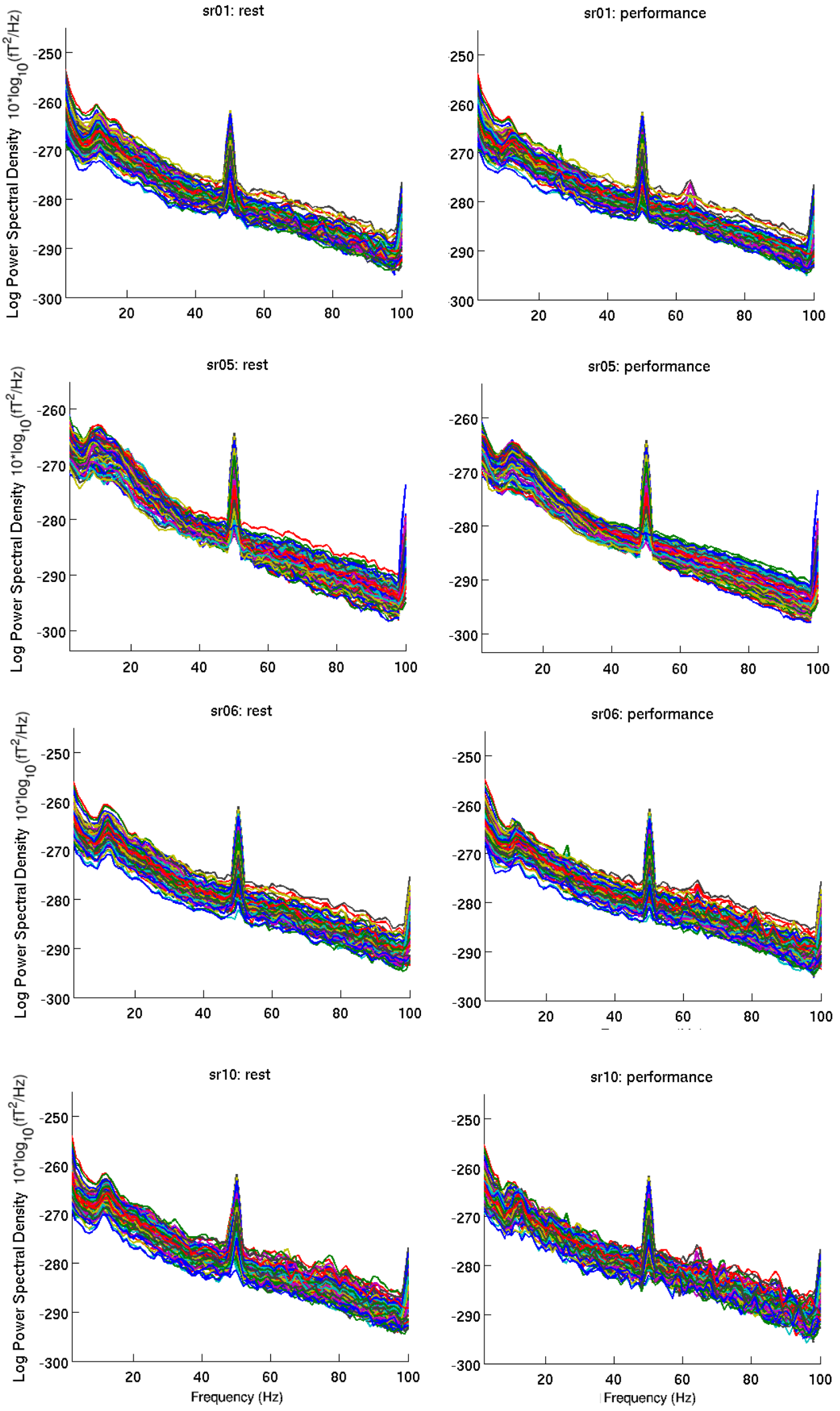
sr01: rest
sr01: performance
sr05: rest
sr05: performance
sr06: rest
sr06: performance
sr10: rest
sr10: performance
Log Power Spectral Density 10*log10(fT2/Hz)
Frequency (Hz)
-250
-260
-270
-280
-290
-300
20
40
60
80
100

Figure S5. Power spectral density (PSD, in units of $10*\log_{10}$ [fT^2/Hz]). The PSD of the magnetometers in the performance blocks was estimated separately for (i) the *resting* periods between performance trials (amounting to approximately 2 minutes per subject; left panels) and (ii) the *performance* trials (15 trials x 23 seconds amounts to 5.75 minutes; right panels). The four rows depict the PSD results for four representative participants with sources localised to the cerebellum. No increase in PSD in the higher frequency range above 20Hz is observed during performance, relative to rest recordings, supporting that there was not a significant contribution of muscle-artifacts to the general level of oscillatory activity. **See Figure S6 for statistical analyses of these effects.** The most notable difference between the PSD during rest and performance was a higher level of alpha (8-13Hz) power at rest, as expected.

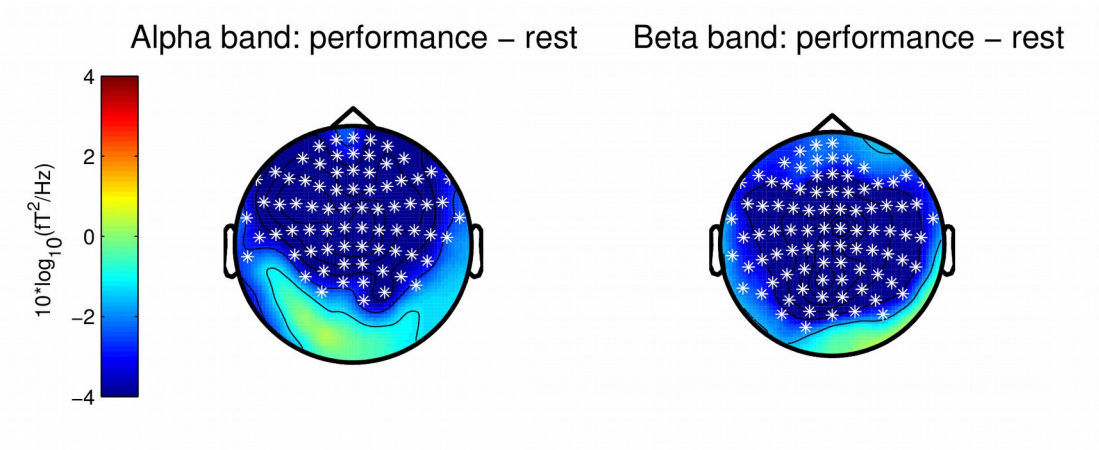

Figure S6. Significant clusters of differences between performance and rest in power spectral density (PSD) in the alpha (8-12Hz) and beta ranges (13-30Hz). Scalp topographies for PSD changes (**in units of $10*\log_{10}$ [fT^2/Hz])**in the alpha (left) and beta (right) frequency ranges, corresponding to the significant clusters obtained (cluster permutation test, $p < 0.025$, two-sided test) for the between-condition comparisons. In both cases a negative cluster was found due to the significantly lower PSD during performance relative to rest. **A similar analysis performed in the gamma range (31-100Hz) revealed only a trend for significance ($p = 0.045$, non-significant in our two-sided test) due to less pronounced gamma power during performance than during rest over parietal and occipital electrodes.**